Electrical Impedance Tomography:
The realization of regional ventilation monitoring

Eckhard Teschner
Michael Imhoff

Dräger. Technology for Life®

Electrical Impedance Tomography: The realization of regional ventilation monitoring

Eckhard Teschner
Michael Imhoff

Important notes

This brochure is for educational purposes only and does not replace the instructions for use. Prior to using the technique of EIT (Electrical impedance tomography) the corresponding instructions for use must always be read and complied with.

Medical knowledge is subject to constant change due to research and clinical experience. The authors of this publication have taken utmost care to ensure that all information provided, in particular concerning applications and effects, is current at the time of publication. This does not, however, absolve readers of the obligation to take clinical measures on their own responsibility.

The use of registered names, trademarks, etc. in this publication does not imply, even in the absence of a specific statement, that such names are exempt from the relevant protective laws and regulations.

CONTENTS

1. Foreword

This booklet accompanies the introduction of Electrical Impedance Tomography (EIT) as a clinical application for monitoring of regional lung function, especially in intensive care patients. In this context, four questions must be answered:

Why introduce EIT as a supplementary imaging technique in medicine?
What information can be gained from EIT?
Which clinical benefits can be expected?
Why did it take about 30 years to develop appropriate clinical devices?

Today, clinicians are accustomed to rapid improvements of high resolution imaging techniques, such as 128-slice CT scanners, f-MRI methods, SPECT or 3D ultrasound scanning. Do we need EIT with its limited local resolution as an additional tool? The principle answer is that EIT, on one hand, provides images based on new and different information, such as electrical tissue properties. On the other hand, EIT can be applied at bedside as a continuous monitoring technique, as it only requires small devices and does not expose patients or users to any ionizing radiation. These opportunities justify the search for application fields in which EIT will help to improve the care of patients.

EIT was introduced in the early 1980s by Barber and Brown. Soon thereafter, a wide spectrum of possible applications in medicine was suggested, ranging from gastric emptying to brain function monitoring and from breast imaging to lung function assessment. Our group, which had the opportunity to work with early system versions, predicted that, based on our own experiences, the greatest medical benefit of EIT would lie in monitoring regional lung function in intensive care patients. Until today, the heterogeneous distribution of lung injury, e.g. in ARDS (Acute Respiratory Distress Syndrome) patients, is only detectable outside the ICU by CT or by

non-localizing techniques such as MIGET (Multiple Inert Gas Elimination Technique). EIT is the only method which can directly show whether closed lung regions can be opened by a recruitment maneuver and be kept open by optimized ventilator settings, all with the aim to minimize the risk of VALI (Ventilator Associated Lung Injury).

Major drawbacks of early EIT systems included their poor sensitivity and susceptibility to signal interference in clinical settings. Acceptable lung tomograms and ventilation images were only achieved using maximal inspiratory and expiratory hold maneuvers which are not applicable in intensive care patients. The images did not provide valid information on the patient's pulmonary status. Most of the research interest in EIT development focused on the extension of the technology towards multi-frequency systems which could deliver special information on tissue properties, on the introduction of new image reconstruction algorithms, or 3D imaging. The less spectacular, yet indispensable, goal of improving signal acquisition quality was not in the centre stage of activities.

The deficits of the existing EIT systems have been the motivation for our group to enhance sensitivity and to make improved EIT systems available for scientific studies on clinical issues. A major advantage was our opportunity for technical development, validation experiments in animals, volunteer studies and research with patients by affiliation of our group to the centre of Anesthesiology and Intensive Care of the University Hospital in Göttingen. These special conditions facilitated EIT development and brought it very close to practical clinical use, as it tied together all the essential factors for improving the technology and developing it further for use in the clinical setting.

A further substantial step was the cooperation with those commercial companies which stood out as leaders in ventilation technology equipment. Even with their commitment to this field and their substantial financial investment, it took many years to improve the system hardware, perform

validation studies and develop simple but reliable software tools for bringing EIT into broad and successful clinical use. The booklet will tell the story of the considerable experience in EIT application and validation in patients in much more detail.

The final assessment of the particularly promising indications of EIT and their establishment in routine clinical work will result from the experience of a critical but constructive community of future EIT users.

by Prof. Gerhard Hellige

D-61-2011

Prof. G. Hellige, born in 1943 in Berlin, was until his retirement in 2008 head of the Department of Anaesthesiological Research at the Centre of Anaesthesiology and Vice Dean of the Medical Faculty at the University in Göttingen.

He was the leader of multiple research projects on experimental and clinical validation of EIT and member resp. head of several executive boards, e.g. the Cardiolab module of the International Space Station ISS and the Committee on Measuring Technology in Medicine at the German Ministry of Research and Technology.

2. Introduction

Acute Lung Injury (ALI) is a very common complication within the population of intensive care patients. It has been shown that mechanical ventilation with ventilator settings which do not suit the individual requirements of the diseased lung can lead to injury of the cellular structures of the lung tissue. As a result, vascular and alveolar permeability increases and interstitial edema formation occurs. Due to the increased weight of the lung, alveolar collapse may predominantly occur in the dependent lung regions, resulting in even more severe arterial hypoxemia [1].

Lung protective ventilation may not only prevent mechanical pulmonary injury but may also reduce the risk of inducing the systemic release of cytokines, which is associated with the development of multi-organ failure [2, 3, 4]. Thus, over the past decades, clinicians have been searching for strategies to optimize alveolar recruitment, maintain an open lung and limit pulmonary overdistension.

However, finding optimal PEEP (Positive End-Expiratory Pressure) and tidal volume settings for the individual patient remains a constant challenge in clinical practice [5, 6].

For more than 30 years, clinicians have been examining various approaches and monitoring devices to guide ventilator management. As the lung of an ALI patient has heterogeneous properties, global parameters reflecting the condition of the lung as a whole have proved to be insufficient to adequately guide lung protective ventilation [7, 8].

CT (Computed Tomography) imaging reveals the underlying problem of treating patients based on global parameters alone. Fig. 1 schematically shows a slice of the lung of an ALI patient with non-ventilated, poorly and hyperinflated lung regions. In order to achieve a more homogeneous
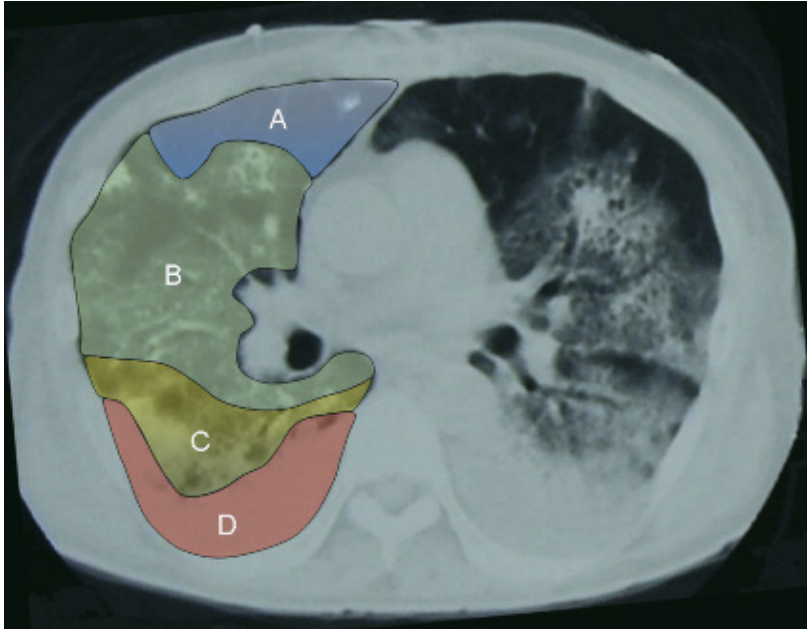
Fig. 1: CT image showing hyperinflated (A), normally aerated (B), poorly aerated (C) and non-ventilated (D) lung regions.

distribution of tidal volume and to keep the lung as open as possible, it has been suggested that therapy settings should be made based on regional information of pulmonary status [9, 10, 11].

Although CT provides detailed regional information about the lung it is, for obvious reasons, not suited for continuous regional lung monitoring at bedside and thus cannot be used to guide the adjustment of ventilator settings performed there.

Electrical Impedance Tomography (EIT) has emerged as a new modality for non-invasive, radiation-free monitoring of regional lung function. With the

Dräger PulmoVista 500, this unique tool is now available as a mature, clinically usable product for the very first time.

Being complementary to well established radiological techniques and conventional pulmonary monitoring EIT can be used to continuously visualize the lung function at the bedside and to assess the effects of therapeutic maneuvers on regional ventilation distribution.

The purpose of this booklet is to provide an overview of the technological and clinical application of EIT, the appearance of EIT images, the parameters that can be derived and the clinical situations that EIT will be used in. The contents and language used were chosen to allow readers without a strong engineering or scientific background to achieve a good understanding of EIT.

As with every new modality, EIT and its clinical application will evolve over time. If this booklet contributes to our understanding of this new approach to lung function monitoring, thereby accelerating this evolution, then its mission will have been successful.
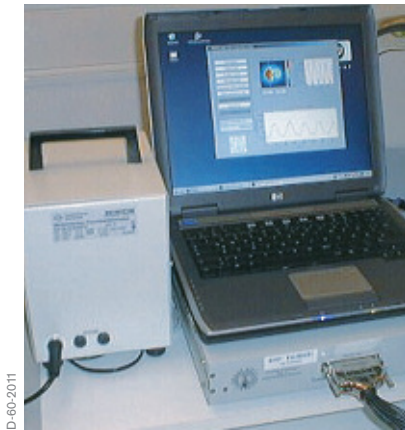
3. The history of EIT
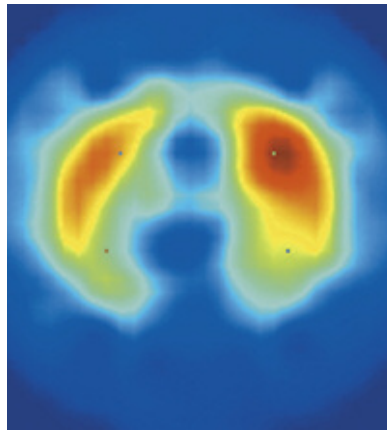

Fig. 2: GOE MF II system

Fig. 3: First EIT image from 2001 taken at Draeger using the GOE MF II

Since the first EIT device (Sheffield Mark I) was developed by Barber and Brown in the early 1980's EIT has received increasing attention within the scientific community. By the mid 1990's more than 30 research groups were actively engaged in EIT related research. The first available EIT devices, although technologically limited, have been applied exemplarily in various scientific fields, including the monitoring of gastric emptying, regional lung monitoring, lung perfusion, cardiac function, neurological function, quantification of lung water and breast cancer screening.

By the mid 1990's the EIT Group in Göttingen, represented by G. Hellige and G. Hahn, had developed a predominantly digital EIT prototype (GOE MF II), which was a further development step beyond the Sheffield Mark I system. It was the world's first EIT system suited for and systematically used in

D-64-2011
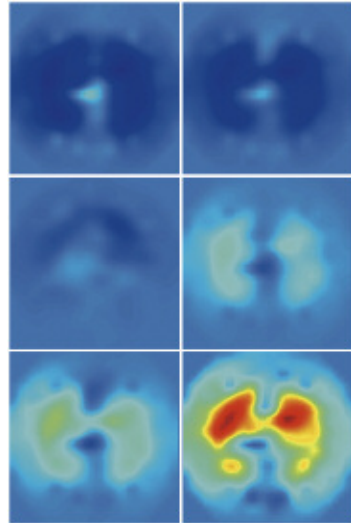
Fig. 4: Early ventilation images made with the GOE MF II

experimental validation studies in animals, physiological studies in volunteers and clinical research. The GOE MF II was specifically designed for the assessment of tidal volume distribution and it was mainly used to evaluate the capability of EIT to monitor regional lung function.

In 2001 the EIT - Group Göttingen and Dräger initiated a scientific exchange of experience in the field of EIT with the mutual objective of improving the technology, design, and software in such a way as to facilitate the use of EIT lung function monitors, not only in experimental research but also in daily clinical practice.

During the initial phase of this cooperative effort, the first major task was to understand why, despite a history of more than 20 years at that time, EIT

Fig. 5: A historic CT Scanner of EMI

D-59-2011

HISTORY OF CT

By way of comparison, Computed Tomography (CT) was invented by G. N. Hounsfield in 1967, a British engineer who worked for EMI (the record label which marketed the Beatles records). The first prototype, dedicated to imaging the brain and completed in 1971, had a resolution of 80 x 80 pixels. The first commercial CT system (SIRETOM) developed by Siemens was launched in 1974. In the following years CT rapidly emerged as a well established diagnostic modality all over the world.

So, the history of computed tomography appears to be only about 10 years older than that of EIT.

Up until the introduction of PulmoVista 500, the use of EIT for regional lung function monitoring has been limited to a growing, but still small, number of experts and research groups. These groups continue to investigate EIT technology within the context of various scientific studies. However, from the today's perspective, it seems that the "path to the Holy Grail" [14] has been much longer than had been initially expected.

had still not found a place in clinical practice, even though the results of all experimental studies had suggested the tremendous potential clinical benefits of EIT when used for regional lung monitoring.

It quickly became obvious that the failure to adopt EIT as a viable clinical tool was closely related to the experience of those who had tried to use it in the clinical setting. EIT devices of that time still were not sufficiently adapted to the "real world" requirements for use in ICUs. This was mainly due to specific limitations in the design of those EIT devices:

D-63-2011

Fig. 6: Application of ECG electrodes in order to perform EIT measurements on an intensive care patient

– Intra-thoracic bioelectric properties are only very slightly changed by ventilation. At the body surface, this results in voltage changes of less than 100µV. In 2001, the most crucial components of EIT devices had only been developed to a point where they could reliably be used in animal trials and healthy humans but not in all intensive care patients. Yet, patients with e.g. lung edema where EIT measurements can be challenging are precisely those who would likely benefit the most from EIT monitoring.

– In previous EIT systems, sixteen single ECG electrodes had to be attached around the patient's thorax and each electrode connected to the corresponding cable. This resulted in preparation times of at least 20 min [15] before EIT measurements could be started. It was apparent that the everyday clinical use required an improved method of electrode application.

– Various EIT software tools had been developed to address scientific questions and identify relevant parameters – but all tools were designed for off-line use and thus did not allow clinicians to perform on-line data interpretation, i.e. directly at the bedside.

EIT EVALUATION KIT 2

In 2006 Dräger had finalized the development of a limited series of EIT prototypes (EIT Evaluation Kit 2). Its design addressed various aspects of the identified obstacles related to data acquisition and clinical usability.

– The electronics for the data acquisition and also the patient cables were completely redesigned to achieve reliable measurements of sufficient signal quality even in those patients with wet lungs and small tidal volumes, where previous EIT systems failed.

– An EIT electrode belt was developed which made electrode application and maintenance much easier. Also, the surface of the electrodes became larger and thus stability of the skin-electrode contact improved so EIT measurements were much more reliable and feasible for larger time periods.

– Additionally, the Dräger MonoLead™ cables that had already been successfully introduced by Dräger for ECG measurements were adapted for use with the newly developed electrode belt. This meant that the cables could be attached to the belt before it was applied to the patient. As with the belt the cable also contributed to a significant improvement of signal quality compared to previously used single lead cables.

– The experience Dräger has in software and user interface design was utilized in the development of software for the EIT Evaluation Kit 2. In contrast to previous EIT systems the EIT Evaluation Kit 2 made the continuous display of EIT images and waveforms possible. The user interface was designed according to principles of the graphical user interfaces of the latest Dräger medical devices at that time.

Fig. 7: Electrode belt of the EIT Evaluation Kit 2 attached to an intensive care patient after abdominal surgery

The EIT Evaluation Kit 2 was limited to use within clinical studies in order to answer the most important question: Could EIT emerge as a tool for routine clinical practice or would its previous limitations cause it to remain a research tool?

In an early evaluation, EIT measurements were performed at 11 hospitals around the world. Results from 183 patients mainly suffering from ALI / ARDS were analyzed. After each EIT measurement clinicians wrote a report which addressed the general usability of the device.

Also, analysis of the collected EIT data revealed, from a technical point of view, that EIT measurements were successfully performed on all patients.

D-47-2011

Fig. 8: EIT Evaluation Kit 2

After 5 years' research experience and following the positive results of these early investigations, Dräger decided to initiate the development of PulmoVista 500 intended to become the first commercially available EIT device dedicated to clinical use. In achieving a high level of clinical suitability Dräger addressed the detailed feedback from more than 30 clinicians from all over the world, who had used the EIT Evaluation Kit 2 for at least several months.

With the launch of the Dräger PulmoVista 500, EIT-based regional lung function monitoring has, following almost 30 years of evolution, finally found its way into routine clinical practice.

4. The principles of EIT as applied by PulmoVista 500

DYNAMIC DETERMINATION OF REGIONAL BIOELECTRICAL PROPERTIES WITHIN THE THORAX

PulmoVista 500 is designed as a lung function monitor for clinical use which continuously generates cross-sectional images of the lung function by applying the technique of electrical impedance tomography (EIT).

To perform bioimpedance measurements, an electrode belt containing 16 electrodes is placed around the chest wall. Additionally, one reference electrode must be attached to a central point on the body, preferably on the abdomen. The reference electrode ensures that all measurements at different electrode pairs are referenced to the same electric potential.

Fig. 9: PulmoVista 500

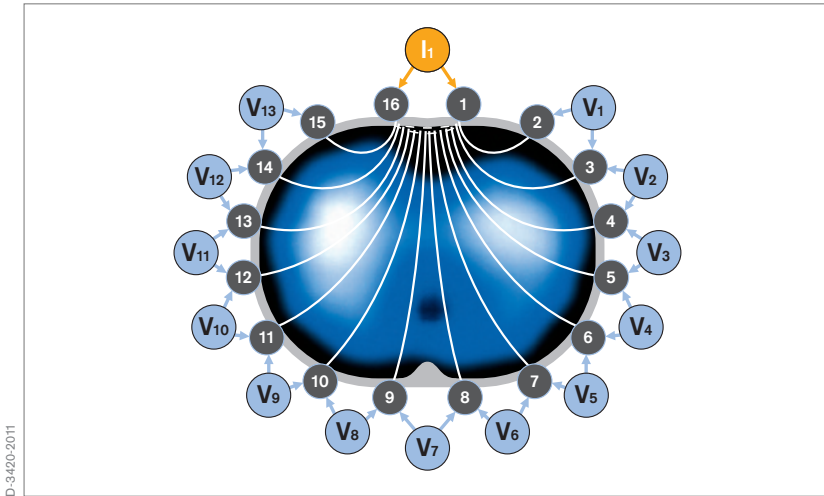Fig. 10: Electrode belt with patient cable connected

Fig. 11: Current application and voltage measurements around the thorax

MEASUREMENT PRINCIPLES

PulmoVista 500 determines the distribution of intra-thoracic bioimpedance by applying a known alternating current "I1" to a first pair of electrodes and measuring the resulting surface potentials "Vn" at the remaining 13 electrode pairs. Applying Ohm's law, the bioelectrical impedance between the injecting and the measuring electrode pairs is determined from the known applied current and the measured voltages. Subsequently, the adjacent electrode pair is used for the next current application and another 13 voltage measurements are performed. The location of the injecting and measuring electrode pairs successively rotates around the entire thorax. One complete rotation creates voltage profiles at 16 electrode positions, each consisting of 13 voltage measurements. The resulting 208 values, also called a frame, are used to reconstruct one cross-sectional EIT image.

Please see Appendix II for more details about bioimpedance measurements.
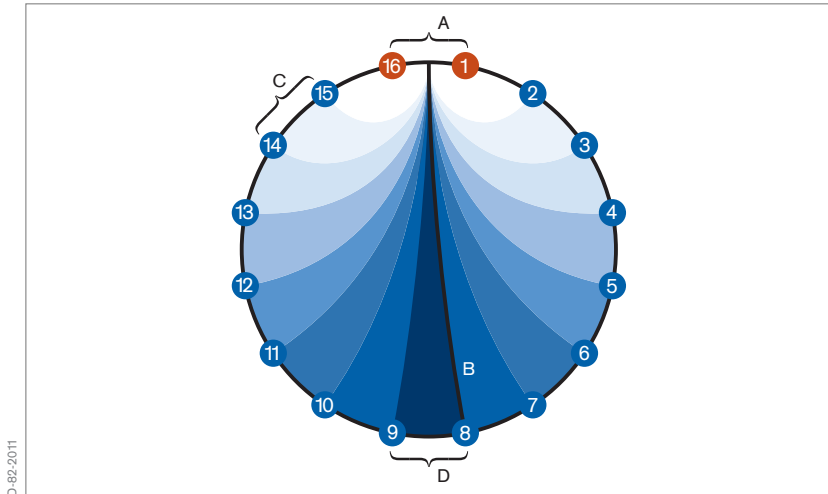
Fig. 12: Distribution of isopotential lines inside the subject. The voltages (C) next to the current application are the highest, as indicated by the white color. The voltage (D) on the side opposite the current application is the lowest, indicated by the dark blue color.

IMAGE RECONSTRUCTION

A current application (A) at the surface of a subject with homogenous bioelectric properties causes a reproducible distribution of potentials inside the subject. The regions in the thorax with the same electrical potential, as a result of current application, are called isopotential lines (B). The distribution of isopotential lines contributes to a predictable voltage profile on the surface of the body.
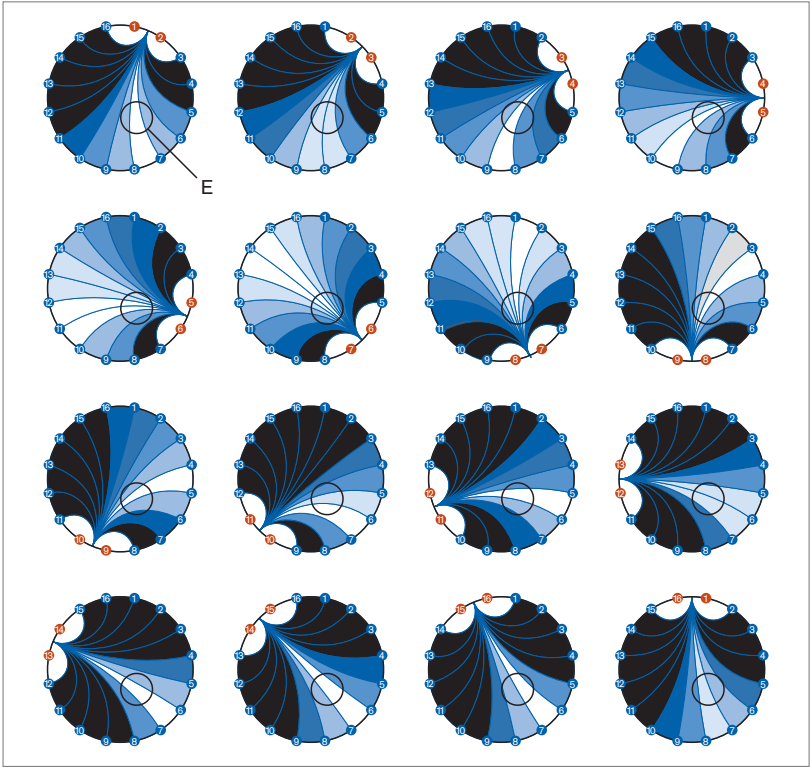
Fig. 13: Profiles of voltage deviations in the presence of a regional increase of impedance. In this figure, white and light blue colors represent deviations of the voltage distribution in an inhomogeneous medium. Voltages without deviation are indicated by the black color.

A regional increase of impedance (E) of the subject results in a change in each of the 16 voltage profiles which make up one frame. Regardless of where the current is applied, the regional increase of impedance always causes an increase of the voltages "behind" the region of increased impedance.

Originally the Sheffield Back-Projection reconstruction algorithm, described by Barber and Brown [16] and drawing on principles similar to those used for computed tomography was developed to compile the recorded voltage profiles into cross-sectional images.

The reconstruction algorithm superposes the 16 voltage profiles on each other (Fig. 14). Reconstruction artifacts are eliminated by applying selective boundary filtering. The resulting image (Fig. 15) displays the region of increased impedance (E) at the correct location.

As with CT scans the projection of the displayed EIT images is from caudal to cranial. This means that the left side of the image displays the right side of the patient. The upper part of the image displays the ventral aspect of the patient.
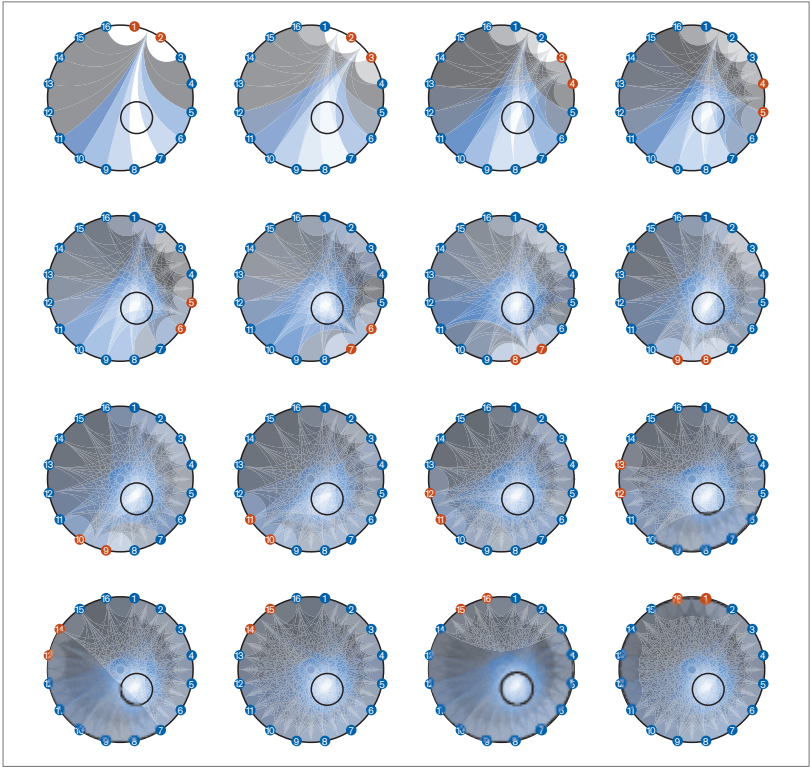
Fig. 14: Successive superposition of the 16 voltage profiles
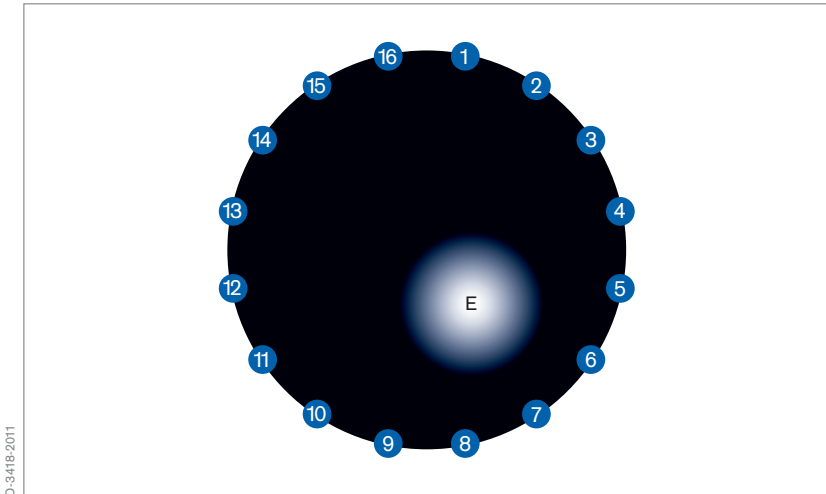
Fig. 15: Resulting image after selective boundary filtering

However, as described by Yorkey et al. [17], the Sheffield Back-Projection reconstruction algorithm carries some inherent limitations, such as a geometry fixed to round shaped subjects, no means to suppress corrupt data and no flexibility regarding the sequence of current injections and voltage measurements. It had since been demonstrated that iterative approximation methods, such as the Newton-Raphson algorithms deliver better results.

For these reasons, PulmoVista 500 uses a Finite Element Method (FEM) based linearised Newton-Raphson reconstruction algorithm to convert the 208 voltages of a frame into an ellipsoid EIT image.

D-3419-2011
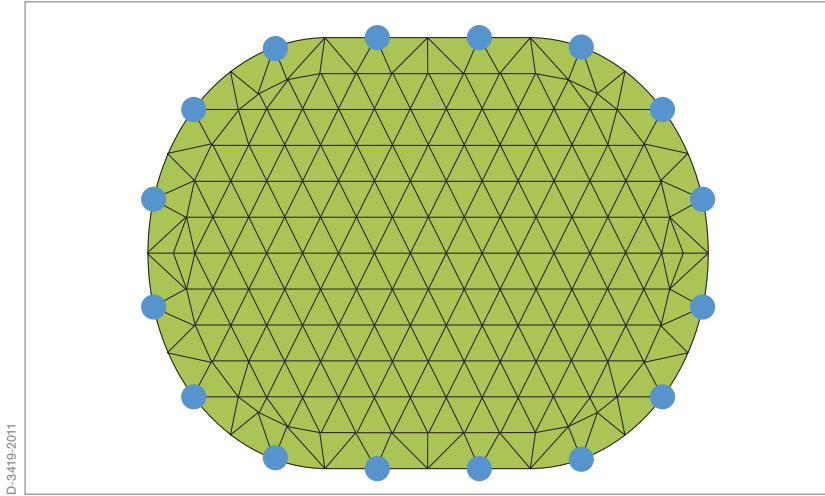
Fig. 16: 2D mesh with 340 finite elements for 16 surface electrodes

This method divides the area within the electrode plane into 340 triangular elements, where each element is assigned homogeneous and isotropic bioelectrical properties.

This method allows the calculation of the resulting surface voltages at the boundary nodes of the model, for any arbitrary distribution of impedance values within this mesh, which is the numerical solution of the so-called "forward problem".
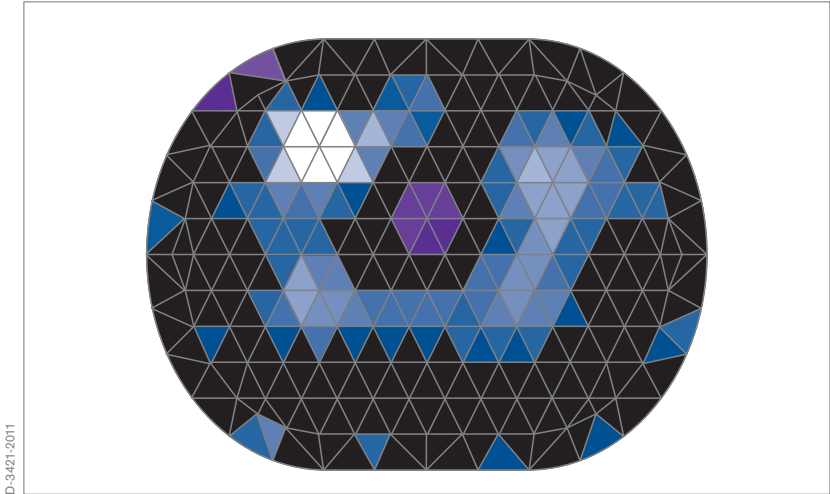
D-3-421-2011

Fig. 17: FEM based reconstruction of regional bioimpedance distribution based on 208 measured surface voltages

For reconstruction of EIT images however, the approach is reversed: after the voltages at the body surface have been measured, their relative changes are fed into the Newton-Raphson reconstruction algorithm by multiplying them with a sensitivity matrix. This matrix has been optimized over the last several years by taking into account real EIT data from several hundred patients.

This algorithm attempts to assign a relative impedance change to each individual finite element to achieve a best match for the numerical solution of this so-called "inverse problem" of the FEM to the actual voltage profile.
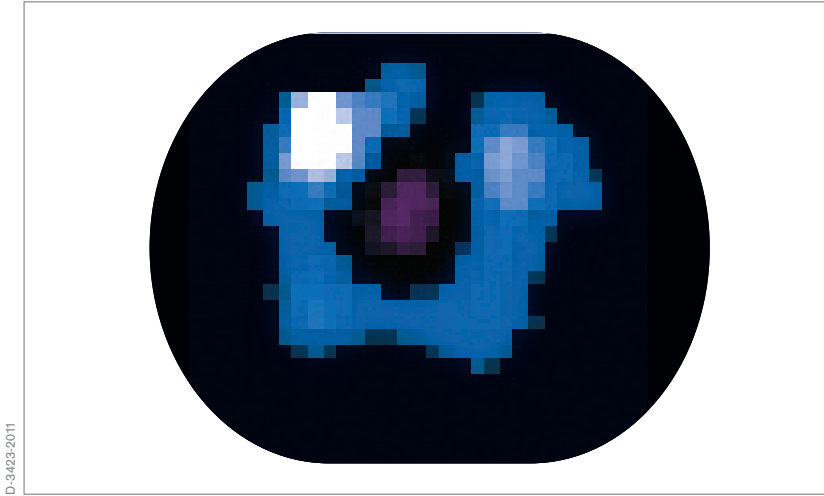
D-3423-2011

Fig. 18: Co-registration and damping of boundary artifacts

Following image reconstruction, the triangular structure is converted into a rectangular pattern ("co-registration") for further image processing. Also, damping of boundary artifacts is applied.
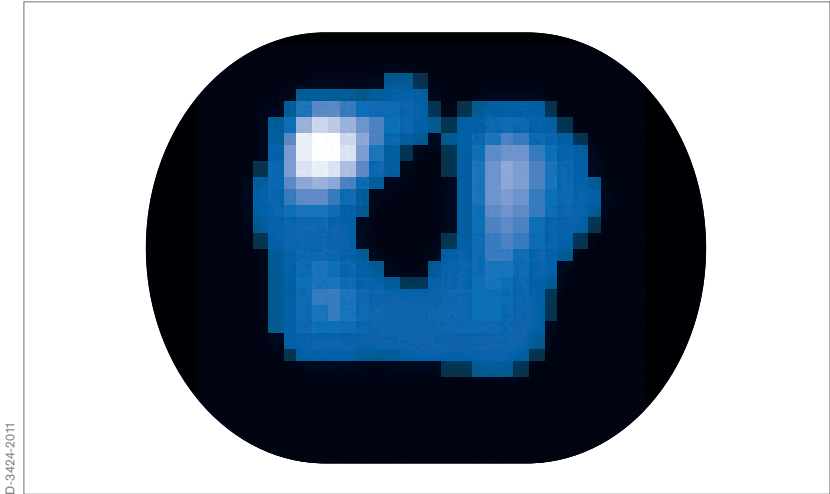
D-3424-2011

Fig. 19: Smoothing by applying Gaussian filtering

In the next step, a Gaussian filter is used to smooth the image. Gaussian filtering is widely used in graphics software, typically to reduce image noise and details. The visual effect of this technique is that of a smooth blur, which resembles viewing the image through a translucent screen. Gaussian smoothing is also widely used as a pre-processing stage in computer vision algorithms in order to enhance image structures at different scales.

D-3425-2011

Fig. 20: Bilinear filtering

Each EIT image consists of a matrix of 32 x 32 pixels. In order to create larger images for better graphical representation and interpretability bilinear interpolation allows to increase the virtual resolution of the EIT images to a matrix of any size, as EIT images in a larger format enable better separation of the displayed structures by the viewer. However, the underlying resolution of the images remains unchanged.
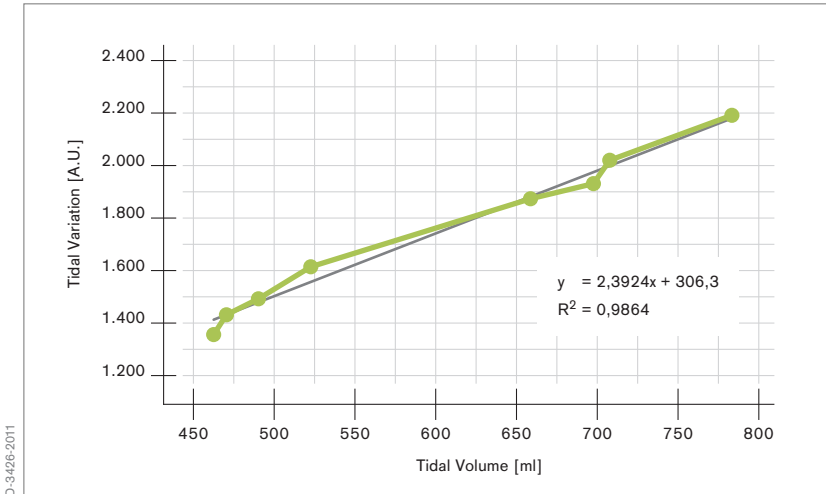
Fig. 21: Correlation of tidal volumes and tidal variations, i.e. ventilation related impedance changes, in a patient with aortic valve replacement after a PEEP reduction from 17 down to 10 cm H_2O

BIOELECTRICAL PROPERTIES OF LUNG TISSUE

As discussed in detail in the Appendix II, it is well known that the impedance of lung tissue varies with the air content. Thus ventilation and changes of end-expiratory lung volume that occur within the electrode plane result in changes of the voltages measured at the body surface.

In humans, an inspiration maneuver from residual volume to total lung capacity amplifies regional bioimpedance by around 300 % [18, 19]. Cardiac activity and perfusion cause a change in thoracic bioimpedance, from diastole to systole, in the range of 3 % [20].

Extravascular lung water, body movement and the skin-electrode resistance may also have various effects on thoracic bioimpedance.

D-3422-2011
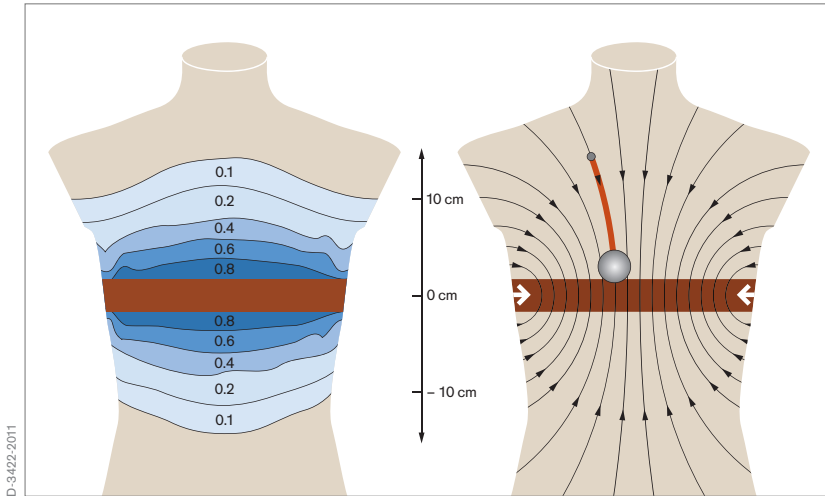
Fig. 22: Left: Contribution of impedance with increasing distance from the cross-section, that is defined by the position of the electrode belt.

Fig. 22: Right: Projection lines of impedance changes within the body; Impedance changes are moved towards the central region with increasing distance from the transversal plane.

THE ELECTRODE PLANE

In the context of EIT, the term "electrode plane" describes the lens-shaped intra-thoracic volume whose impedance changes contribute to the generation of EIT images.

The actual thickness and the shape of this electrode plane depend on the dimensions, the bioelectric properties and the shape of the thorax, and particularly on the morphological structures inside of it. Further, the degree of homogeneity of trans-thoracic bioelectric properties also has an effect on the dimension of this electrode plane.

The electrode belt used with PulmoVista 500 uses electrodes which are 40 mm wide. Hence, close to the body surface the electrode plane is at least 40 mm thick. The thickness of the plane increases towards the central region of the body. The contribution of impedance changes is reduced with increasing distance from the cross-sectional plane (Fig. 22 left). Increasing distance from the cross-sectional plane moves the position of impedance changes close to the body surface, towards the central region along the depicted projection lines (Fig. 22 right). However, as the contribution of impedance changes is reduced with increasing distance from the cross-sectional plane, the effect on the image is limited.

FUNCTIONAL EIT

PulmoVista 500 performs functional EIT, meaning that it mainly displays relative impedance changes as a result of lung function, i.e., ventilation and changing end-expiratory lung volume. If the signals are not filtered, cardiac related impedance changes are also displayed. Factors affecting the absolute impedance are eliminated by only displaying relative impedance changes, rather than absolute impedance values.

Thus, the Dynamic Images generated by PulmoVista 500 contain information on the functional condition of different lung regions within the electrode plane.

5. Clinical information derived from PulmoVista 500

D-87-2010

Fig. 23: PulmoVista 500 in a clinical setting

PulmoVista 500 is the first EIT system of its kind which continuously provides graphical information about the regional distribution of ventilation and changes of end-expiratory lung volume. The temporal resolution of this information is high and it can even be presented as trend data. While this opens up a number of new approaches to observe specific conditions of different lung regions, it generally also carries the risk that the information provided by EIT devices may be too complex to be used by clinicians who have limited experience in this field.

With reference to EIT measurements it is important to remember the terms "distribution of ventilation" or "lung volume changes" refer to physiological processes inside the previously described electrode plane, i.e. the lens-shaped

D-46-2011
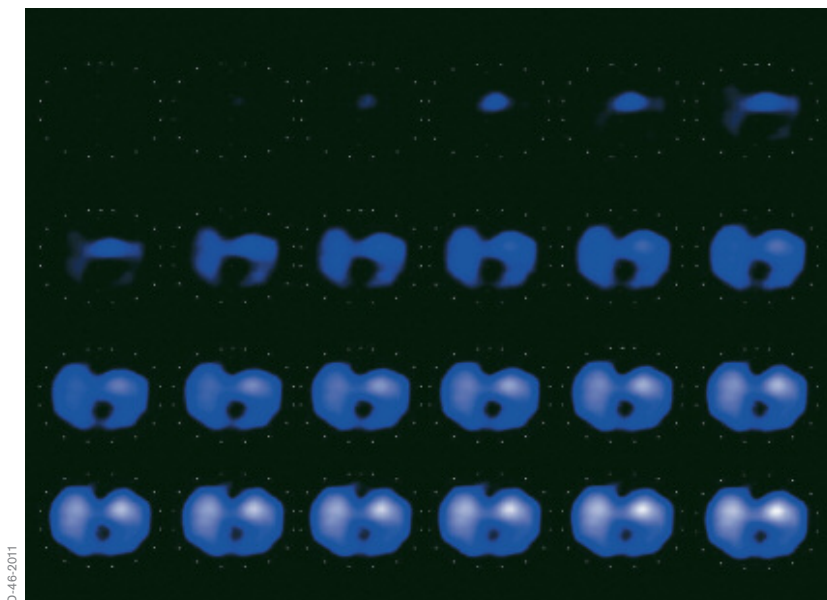
Fig. 24: Series of dynamic images representing air filling during inspiration

intra-thoracic volume. PulmoVista 500 captures a relatively thick slice of the lung which might represent about 10 % to 30 % of the entire lung.

5.1 SCREEN ELEMENTS DISPLAYED BY PULMOVISTA 500

DYNAMIC IMAGE

The Dynamic Image continuously displays relative impedance changes within the electrode plane as a movie which represents the dynamics of ventilation. PulmoVista 500 can generate up to 50 EIT images per second. This high temporal resolution facilitates the visualization of regional ventilation even at higher respiratory rates. For example, when
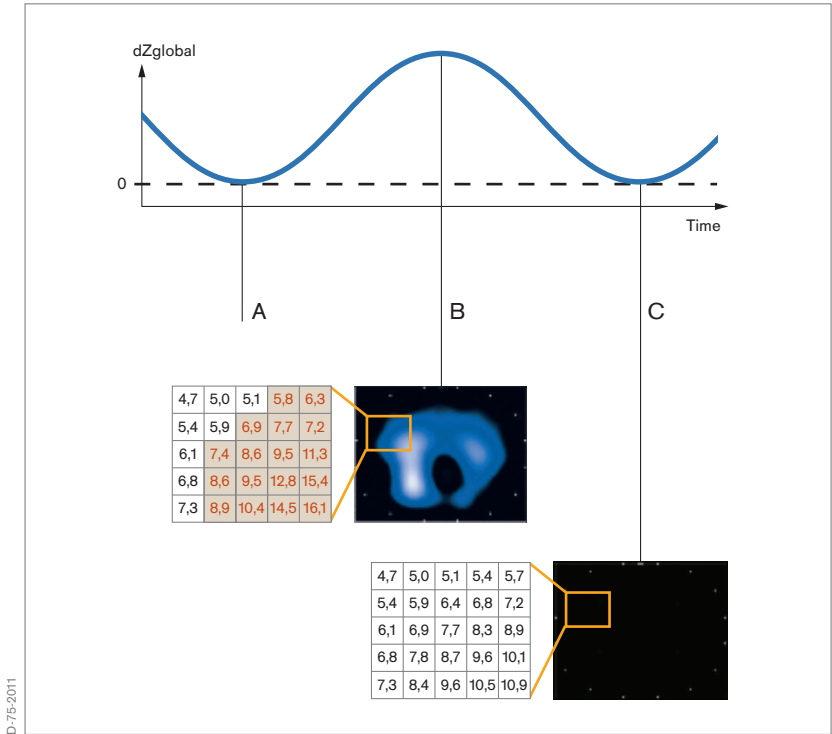
Fig. 25: Generation of EIT images

PulmoVista 500 uses a frame rate of 20 images per second and the respiratory rate is 30 breaths per minute 40 EIT images per breath will be generated.

Each EIT image is determined by referencing the current frame (B), i.e. the set of 208 voltages, to a baseline frame (A) which represents the end of expiration of the last detected breath. This results in a frame of relative voltage deviations which then is used for the image reconstruction.

This means that, regardless of the actual values of the baseline frame (which also reflect a certain distribution of absolute impedance), only regional differences between the current frame and the baseline frame are displayed.

If the end-expiratory impedance distribution of the next breath is identical to the former one, the next end-expiratory image (C) is black. As the baseline frame is continuously updated following each detected breath, mainly impedance changes due to tidal ventilation are displayed. Due to this baseline definition, waveform offsets caused by changes in end-expiratory lung impedance are not displayed in the Dynamic Image.

This behavior is somewhat comparable to the volume waveform of a ventilator, which is calculated from the flow waveform and requires calibration to zero after each detected breath. In the ventilator, the volume waveform is zeroed because the external flow sensor cannot distinguish between differences between inspiratory and expiratory volumes either due to leakages or those caused by changes in FRC.

STATUS IMAGES

Further analysis of the lung regions, e.g. comparative evaluation at different times or quantification of regional ventilation distribution, can be achieved using status images. With PulmoVista 500, the status image can be configured as either a Tidal Image, or as a Minute Image.

The Tidal Image is a differential image of the end of inspiration compared to the beginning of inspiration which represents the regional distribution of ventilation of the last detected breath. The Tidal Image is automatically updated after each breath.

The Minute Image represents regional impedance distribution changes as averaged Tidal Images over the last minute. The Minute Images is ideal for the assessment of regional distribution during ventilation with varying tidal volumes.

REGIONS OF INTEREST

A region of interest (ROI) is a user-defined area within a status image. The image can be divided into 4 ROIs of equal but user defined size, either horizontally or into quadrants. The area covered by each ROI is represented by the corresponding regional impedance waveform and the regional numeric value.
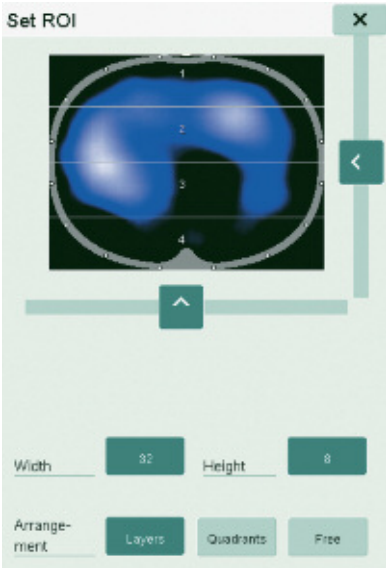
D-43-2011

Fig. 26: An arrangement as "Layers" allows assessing the effects of gravity and thus the different properties of dependent and non-dependent lung regions.

This arrangement helps to assess the effects of e.g. PEEP changes, recruitment maneuvers and to monitor any pathology which equally affects both sides of the lungs.
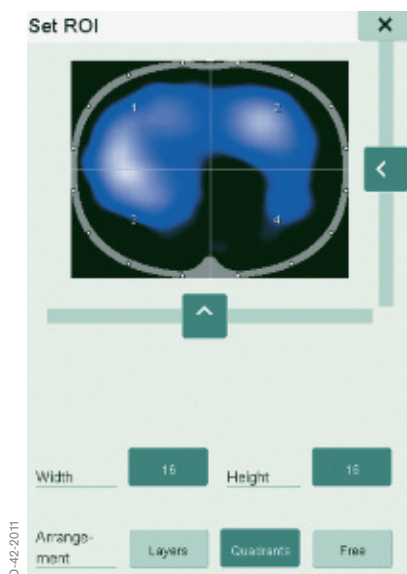
Fig. 27: An arrangement as "Quadrants" allows assessing regional characteristics of the upper and lower left lung vs. the upper and lower right lung.

This arrangement helps to assess the effects of e.g. lateral positioning, lung suction, pleural drainages and to monitor any pathology which affects both sides of the lungs differently.
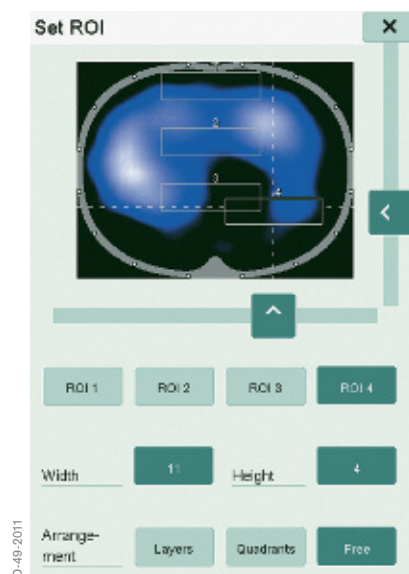
Fig. 28: An arrangement in the mode "Free" allows assessing status images pixel by pixel and to compare non-adjacent lung regions.

D-76-2011
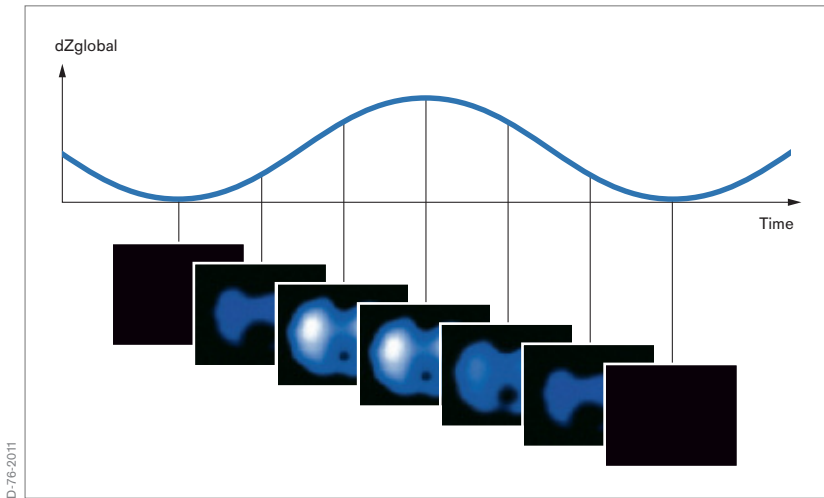
Fig. 29: Generation of the global impedance waveform

IMPEDANCE WAVEFORMS

The status images present the ventilatory status in a somewhat compressed fashion. The temporal behavior of the lung regions cannot be assessed just by interpreting those images.

In contrast, the impedance waveforms represent the impedance changes within the electrode plane over time. All displayed impedance waveforms, i.e. one global and four regional waveforms are plotted simultaneously over the same time base. The impedance waveforms can be assessed in a manner similar to the assessment of waveforms on the ventilator.

The global impedance waveform represents the sum of relative impedance changes in all pixels of each Dynamic Image plotted over time.
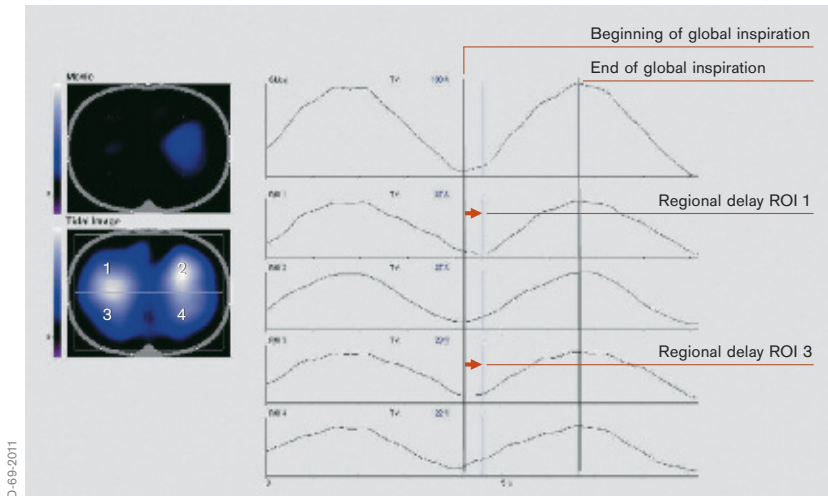
Fig. 30: Impedance waveforms from an individual with delayed air filling in the right lung (ROIs 1 and 3). The dynamics during inspiration in the lung regions can only be seen in the waveforms, and not in the Tidal Image.

The global impedance curve primarily displays impedance changes related to ventilation. There is usually a strong correlation between this curve and the volume curve displayed by the ventilator.

In contrast to the global impedance curve, the four regional impedance curves display the sum of impedance changes within the specified ROI over time. The regional impedance curves allow comparison of impedance changes in different lung regions with respect to this temporal behaviour.

In patients with inhomogeneous pulmonary conditions, the shape and potential phase lags of impedance waveforms provide information about regions with delayed air filling. Also, changes of regional conditions can be analyzed in detail over a longer period of time, depending on the selected time scale.

The parameter Tidal Rate, determined from the global impedance curve, typically represents the number of breaths detected per minute.

The parameter TV global (Tidal Variation global) represents the difference between the minimum and maximum value of the global impedance curve for each breath. The TV global is always 100 %, regardless of the tidal volume. It serves solely as a reference for the display of regional tidal variations.

The regional Tidal Variation TV ROIn represents the difference between the minimum and maximum values on the regional impedance curves for each breath, i.e. from end of expiration and the end of inspiration.

End of expiration and inspiration are detected on the global impedance curve and indicated by markers. Regional Tidal Variations show the percentage of impedance change which takes place in the corresponding ROI.

Fig. 31: Numeric values of PulmoVista 500

D-3429-2011

NUMERIC VALUES

Numeric values are continuously calculated and displayed so that quantification and comparison of regional impedance changes at different times is possible. PulmoVista 500 uses a very straightforward method to express distribution of ventilation in the electrode plane – it simply expresses the distribution within the electrode plane as regional proportions.
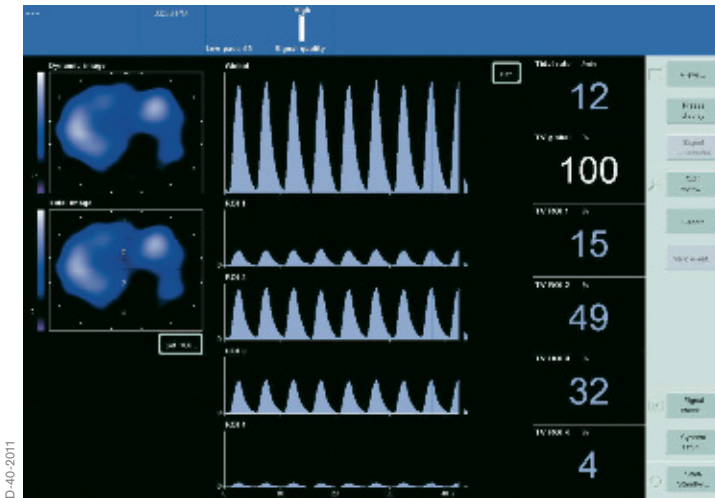
Fig. 32: Screenshot "Main" view

5.2 MAIN VIEW

The "Main" view is the usual monitoring screen and displays the following:
A "Dynamic Image", showing impedance changes over time, a "Status Image", a
global impedance waveform at the top, and below this, four regional impedance
waveforms, representing relative impedance changes of the Regions Of
Interest (ROI) defined in the "Status Image". On the right side of this screen,
parameter fields are arranged which contain the numeric values described.

Based on the feedback provided by more than 30 clinical users of EIT over
several years it had become increasingly obvious that the best way to present
EIT data is to combine EIT status images (containing regional information),
impedance curves (containing regional and temporal information) and
derived numerical parameters (allowing quantitative assessment).
Consequently, the "Main" view of the PulmoVista 500 provides EIT data in a
graphical layout similar to that which clinicians know from patient monitors.

D-45-2011
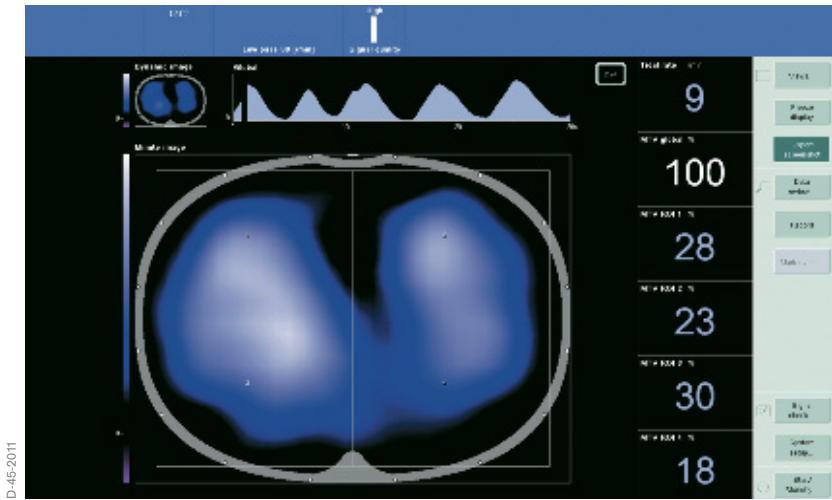
Fig. 33: Full Screen Image view

5.3 FULL SCREEN IMAGE VIEW

The view "Full Screen Image" displays contents similar to the "Main" view. However, by providing a large format view of either the Dynamic Image or a status image it allows users to easily snatch an impression of ventilation distribution from a remote position. Thus this view might be especially helpful during clinical rounds, during training or in other situations when the presentation of EIT images in front of a larger group of people is required.
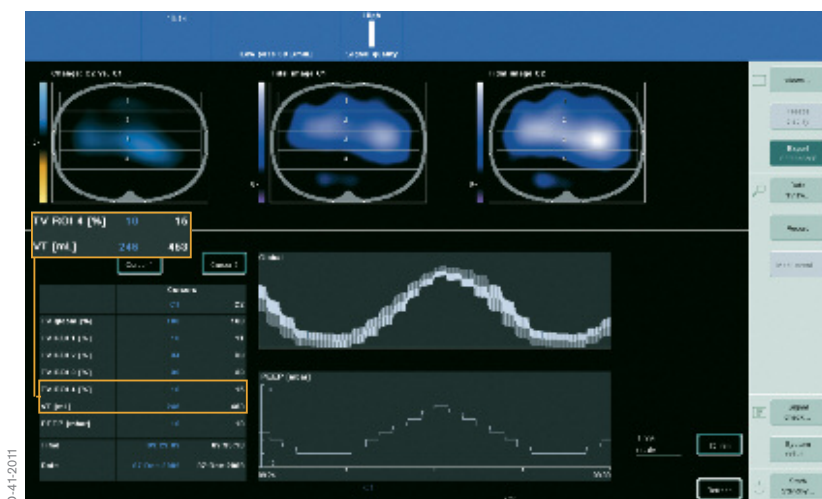
Fig. 34: "Trend View", showing an example of trended distribution of ventilation during an incremental and decremental PEEP ramp (PCV) in an experimental trial (30 kg piglet). Comparing the distribution of ventilation at a PEEP of 10 mbar in the incremental and decremental part of the PEEP ramp reveals redistribution towards the dorsal lung regions (the trend table shows an increase of TV ROI 4 from 10 % to 15 %), while the tidal volume (via Medibus from the ventilator) increased from 246 ml to 453 ml. The differential image (on the left, "Change: C2 vs. C1") shows in a turquoise color lung regions where this increase mainly occurred.

5.4 TREND VIEW

While a single status image provides an impression of the homogeneity of ventilation and which lung regions may be not ventilated at all, the major clinical use and added value when compared to radiological images comes from the ability of PulmoVista 500 to compare and assess EIT status images before and after therapeutic interventions.

The trend page provided by PulmoVista 500 allows continuous display of two status images generated at different times. Regional ventilation distribution

can thus be reviewed over a time period of up to 120 minutes. Two cursors can be easily navigated through the global impedance curve: an additional image, reflecting the difference between the status images at each cursor position displays regional changes associated by changed lung conditions or by a change of therapy.

If a Dräger Evita family ventilator is connected to PulmoVista 500 via the Medibus interface, ventilation parameters such as PEEP, which can affect regional distribution, can also be displayed in this view.

5.5 ΔEELI TREND VIEW

It is well known that not only ventilation affects the intra-thoracic impedance but also changes of the End-Expiratory Lung Volume (EELV).

In order to continuously display the impedance changes due to ventilation, all offsets induced by changes of EELV and concurrent changes of End-Expiratory Lung Impedance (ΔEELI) are suppressed in the Main view by referencing all impedance values to a dynamic baseline.

Nevertheless, the ability to continuously display ΔEELI on a regional level provides further information which is potentially as useful as the display of regional ventilation. Continuous information about ΔEELI is especially suited to assess the dynamics of slow recruitment and derecruitment processes within the lungs. Not surprisingly, the early users of EIT devices had consistently asked for a means with which to assess ΔEELI.

Therefore the ΔEELI trend view, dedicated to the display and quantification of global and regional changes in end-expiratory lung impedance over time, has been implemented in PulmoVista 500.

The ΔEELI trend displays a differential image "ΔEELI: C2 vs. C1", which represents the difference between end-expiratory images at the two cursor positions C1 and C2.

Up to 20 minutes of global and regional impedance waveforms are displayed, which are referenced to a fixed baseline. Parameter fields display the numerical parameters ΔEELI global and four ΔEELI ROI. The numeric value ΔEELI global displays the deviation of the global end-expiratory status at the cursor positions C1 and C2 in relation to the global tidal variation at C1. The numeric value ΔEELI ROI displays the regional deviations within the respective ROI.
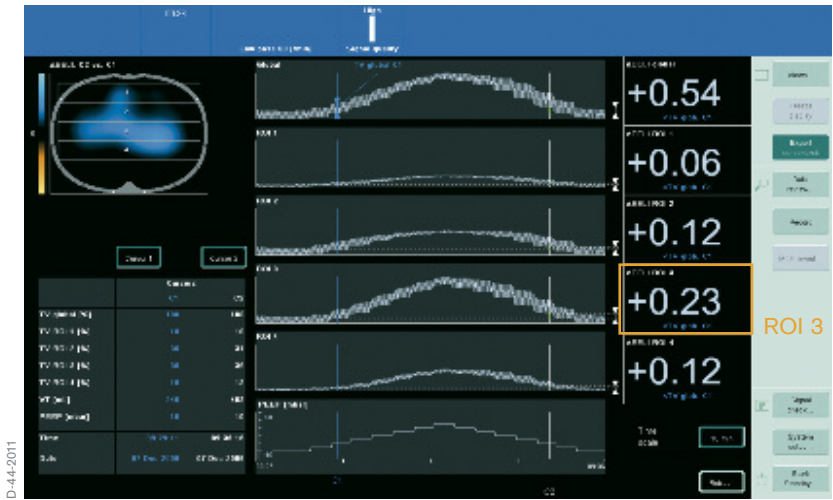
Fig. 35: Trended distribution of ΔEELI during an incremental and decremental PEEP ramp (PCV) in an experimental trial (30 kg piglet). Comparing the distribution of end-expiratory lung volumes at the same PEEP levels in the incremental and decremental part of the PEEP ramp reveals an increase of ΔEELI especially in the dorsal lung region ROI 3 (as displayed in the parameter fields). The differential image "ΔEELI: C2 vs. C1"depicts in turquoise color, the lung regions where this increase of EELI occurred.

The change in end-expiratory lung impedance ΔEELI at C1 and C2 is expressed as follows:

Zero change: no difference between values at C1 and C2
Positive changes: value at C2 is greater than the value at C1
Negative changes: value at C2 is less than the value at C1

A positive change in ΔEELI global of 1.00 * TVglobal C1 indicates an increase in end-expiratory lung impedance equal to the global tidal variation (at C1), which in turn is related to the tidal volume located within the electrode plane.

6. Clinical applications of EIT

As discussed above EIT provides a means of visualizing the regional distribution of ventilation and changes of lung volume. This ability is particularly useful whenever there is a need to improve oxygenation or CO_2 elimination and when therapy changes are intended to achieve a more homogenous gas distribution in mechanically ventilated patients.

Today, the assessment of regional gas distribution can only be based on CT or MRI scans. However, CT involves exposure to significant doses of ionizing radiation [21, 22]. Also, CT and MRI are usually not performed at the bedside and thus require that the patient is transported to the radiology department. The intra-hospital transport of critically ill ventilated patients represents a significant risk for the patient and increased workload for caregivers.

Moreover, CT and MRI images are static and thus only represent lung volume at one point in time. Also, CT and MRI cannot provide real-time quantification of air content in predefined ROIs. Even though CT provides images of the regional gas distribution, experts do not consider CT to be suitable for the optimization of ventilation settings.

Due to the general properties of EIT and the specific design of PulmoVista 500 it can easily be used continuously at the bedside and provide information about distribution of ventilation as well as changes of end-expiratory lung volume.

No side effects of EIT have ever been reported. Besides the unique information provided by EIT, its convenience and safety contribute to the increasing perception expressed by various authors that EIT has the potential to be used as a valuable tool for optimizing PEEP and other ventilator settings [23, 24].

The effects of various therapeutic treatments have already been assessed with the help of EIT, and this chapter gives an overview on the literature that has been published in this context.

PEEP TITRATION

It is likely that the titration of PEEP will be one of the primary motivations for the use of EIT.

Currently, there is no consensus within the medical community on how to optimize ventilator settings such as PEEP. Knowledge about the distribution of ventilation could help the clinicians to set ventilation parameters more appropriately for the individual patient and thus potentially reduce ventilator associated lung injury (VALI).

EIT based titration of PEEP to avoid atelectasis on the one side and regional hyperinflation on the other side has already been described by Hinz [25]. Hinz also interpreted the "filling characteristics", where local impedance waveforms are plotted over global waveforms where he found significant differences between dependent and non-dependent lung regions. In the same publication the ability to find regional upper inflection points in regional pressure-impedance curves was established; this can be used to assess a wide variety of PEEP trials.

Amato MB, presented a method which aimed at achieving a 1:1 ratio of ventilation, in the upper and lower halves of the lung respectively, postulating that this approach would achieve the most homogeneous distribution of ventilation. He suggested performing a decremental PEEP trial to establish this ratio based on EIT data.

Erlandson et al. [24] assessed the development of the end-expiratory lung impedance at different PEEP settings over time; it was hypothesized that a constant level of EELI would correspond to a stable end-expiratory lung volume (within the electrode plane) and thus would indicate the optimal PEEP setting.
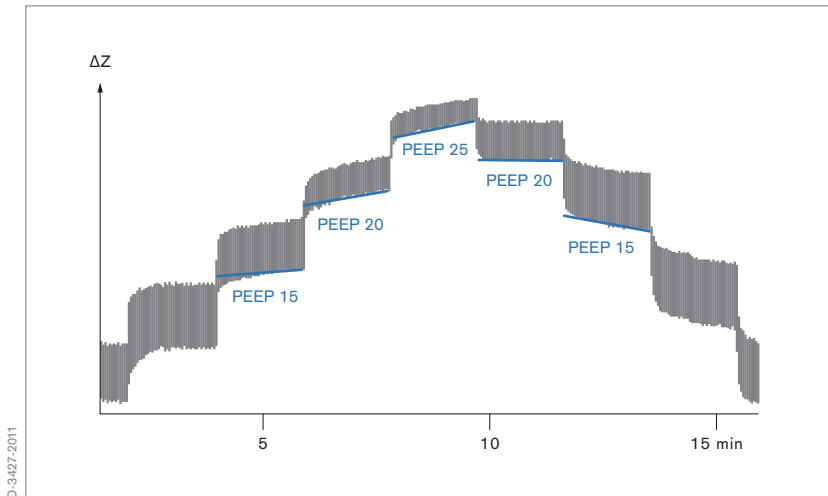
Fig. 36: Defining optimal PEEP settings based on the assessment of ΔEELI

Muders et al. [26] described an index of homogeneity of regional lung mechanics, the regional ventilation delay (RVD) index. Based on this RVD index, RVD-maps can be generated and the standard deviation of RVD (SDRVD) determined which describes the variation of regional delays of the beginning of inspiration compared to the global beginning of inspiration during a slow inflation maneuver.

Preliminary data show that there is an excellent correlation of SDRVD with cyclic opening and closing, suggesting that this index could also be a promising approach to titrate PEEP settings.
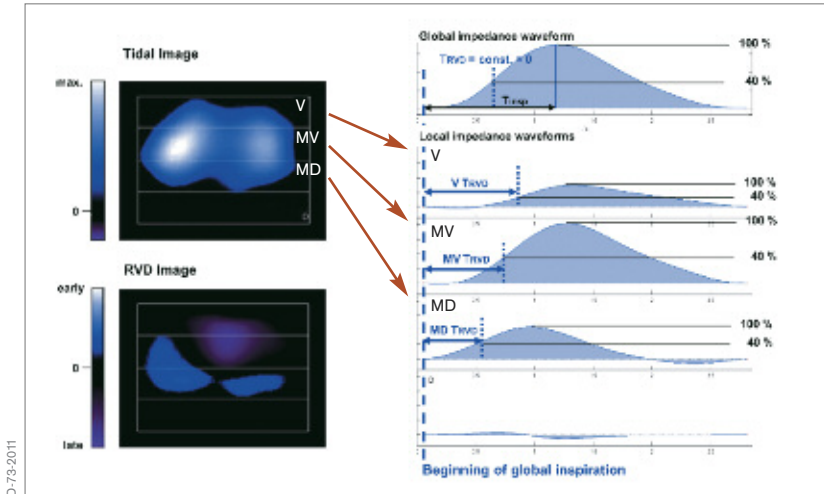
Fig. 37: Distribution of regional ventilation delay in a COPD patient: While the Tidal Image represents the distribution of ventilation, the RVD approach determines the phaselags of beginning of regional inspiration relative to the beginning of global inspiration. This image illustrates why the concept of ROIs is not optimal for RVD analysis: In the mid-ventral (MV) region, the corresponding waveform only shows a slightly delayed beginning of inspiration. However, the RVD Image, in which the delay is displayed for each pixel reveals that the MV region contains regions with early and late opening. A completely black RVD Image indicates a homogeneous beginning of inspiration, purple regions indicate a delayed and blue regions an early beginning of inspiration (preliminary color scale).

ASSESSMENT OF RECRUITMENT MANEUVERS

Recruitment maneuvers aim at reopening collapsed lung regions, thus improving pulmonary aeration and reducing mechanical stress during subsequent ventilation. The regional effects of recruitment maneuvers can be visualized and assessed with EIT [10, 27].

Odenstedt et al. evaluated the effects of different lung recruitment maneuvers with EIT in fourteen animals with induced lung injury [28].

This study confirmed that EIT is capable of continuously monitoring lung volume changes and that EIT can help to identify responders to recruitment maneuvers.

Slow de-recruitment after recruitment maneuvers, caused by insufficient post maneuver PEEP levels, can also be identified.

SPONTANEOUS BREATHING

Frerichs [29] performed EIT studies in infants and concluded that EIT is capable of displaying the effect of spontaneous breathing on the distribution of ventilation.

Putensen [30] presented a case of an intubated patient with acute respiratory failure breathing spontaneously with APRV. When spontaneous breathing in this patient was discontinued ventilation in the right dorsal region almost disappeared, indicating that during mechanical ventilation regional ventilation was predominantly redistributed to the ventral lung areas. Even though these effects are well known and the positive effects of spontaneous breathing on gas exchange, particularly in the dorsal regions, are widely accepted, witnessing the disappearance of dorsal ventilation in association with sedation should provide valuable information for making clinical decisions.

MONITORING OF DE-RECRUITMENT FOLLOWING SUCTIONING PROCEDURES

Endotracheal suctioning is a very common procedure to remove secretions from the airways of intubated and mechanically ventilated patients. While this procedure is often inevitable, it carries the risk, especially in ALI or ARDS patients, of lung de-recruitment, further compromising gas exchange. Using EIT, it has been shown that in some patients, a relatively long period of time passes before end-expiratory lung impedance is restored to levels observed prior to airway suctioning. Lindgren [31] used EIT in an experimental setup to assess lung volume and compliance changes during open and closed suctioning and was able to confirm that EIT is capable of monitoring rapid lung volume changes such as those induced by endotracheal suctioning. These results were replicated in a subsequent clinical study by the same group [32] where the effect of endotracheal suctioning on pulmonary aeration was investigated in ventilated ICU patients. They were able to monitor the derecruitment, as a direct result of suctioning, as well as the slow recruitment that occurred afterwards in some patients.
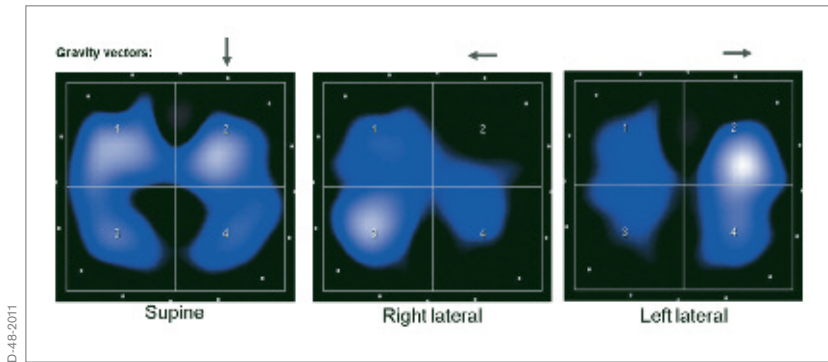
Fig. 38: Redistribution of ventilation in a healthy volunteer; While a typical left / right distribution of 52 % / 48 % is seen in supine position, in a right lateral position this ratio changed to 72 % / 28 %, in a left lateral position to 35 % / 65 %.

MONITORING THE EFFECTS OF PATIENT POSITIONING

Changes in body position of healthy, spontaneously breathing individuals are associated with a major redistribution of regional ventilation. Typically much more ventilation occurs in the dependent lung (the lower lung in a lateral position) than in the non-dependent lung. This is because at the end of expiration, the gravity causes the dependent lung to be more compressed than the upper lung, however, in a healthy individual the dependent lung is fully inflated at the end of inspiration. This means that larger changes of air content occur in dependent regions.

While these phenomena are well known and quite intuitive in clinical practice, EIT allows visualization and assessment of these dynamic changes at the bedside.

D-74-2011
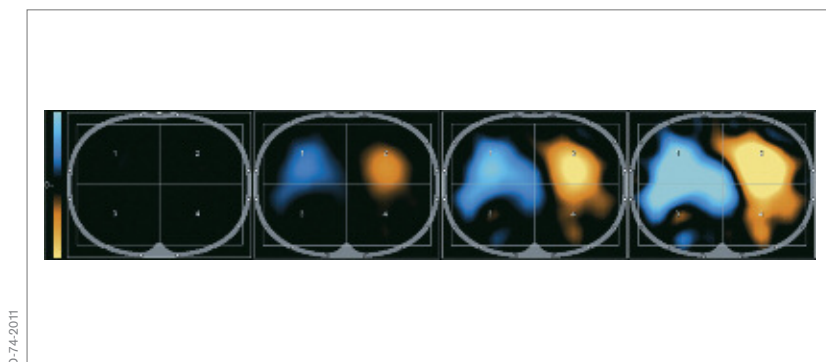
Fig. 39: Changes of end-expiratory lung volume – assessed with the ΔEELI trend view of PulmoVista 500 – in a chest trauma patient in a rotation bed, while being turned from a 60° right lateral (1st image taken at cursor position C1, representing the reference status) to supine position. The images depict how End-Expiratory Lung Volume (EELV) increased in the right (initially dependent) lung during the rotation (blue color), while EELV decreased by a similar magnitude in the left lung (orange color). Despite the large changes in EELV, the distribution of ventilation in this patient did not change significantly during the rotation.

In the last few years prone positioning has been used increasingly in the treatment of ARDS patients [33, 34]. EIT may help monitor ventilation change due to such changes of position. Moreover, it may help identify to responders to this kind of treatment. It may also help identify the best body position in case of a highly uneven distribution of ventilation [35, 36].

POSITIONING OF DOUBLE LUMEN ENDOTRACHEAL TUBES

Steinmann [37] used EIT to assess the correct placement of double lumen endotracheal tubes (DLT) and compared the findings with those obtained using fiberoptic bronchoscopy (FOB). While EIT enables immediate recognition of misplaced left-sided DLTs, EIT did not provide a method to detect incorrectly positioned endobronchial cuffs (as diagnosed by FOB). Thus, EIT cannot replace FOB as a means of determining correct placement of DLTs.

Nonetheless, the authors stated that EIT could be used as an additional tool, complementing auscultation as a non-invasive method of assessing DLT placement.

7. Indications and contraindications

INDICATIONS

PulmoVista 500 is designed to perform thoracic bioimpedance measurements by applying the technique of electrical impedance tomography (EIT). PulmoVista 500 displays regional information on ventilation-related changes of air content within the electrode plane.

While PulmoVista 500 does not provide absolute values for end-expiratory lung volume, it does display regional information on short-term changes of end-expiratory lung volume within the electrode plane.

PulmoVista 500 can be used during mechanical ventilation, mask ventilation and spontaneous breathing.

PulmoVista 500 is intended for use on intensive care patients, whose regional (lung) volume distribution is of clinical interest. The electrode belts used with the device has been designed for the use in recumbent patients in supine, lateral or even prone positions.

Generally speaking, in order to perform EIT measurements the subject can be in an upright, sitting, or supine position, as long as there is no excessive movement during the measurements. Measurements of seated or standing patients may only give satisfactory results when the patient leans against a backrest as some electrodes may, depending on the shape of the posterior muscular structures (latissimus dorsi), not have sufficient skin contact. If required, the belt must be sufficiently secured with adhesive tape during measurements in an upright position.

Due to the fact that EIT monitoring is primarily beneficial in the treatment of patients with severe respiratory complications, PulmoVista 500 is intended for stationary use, at the bedside, in clinical environments and on recumbent intensive care patients.

In principle, EIT measurements can be performed on a wide range of the adult patient population, but also on pediatric and even neonatal patients.

The range of electrode belts which are currently provided with PulmoVista 500 allows EIT measurements on patients with a chest circumference from 70 cm (27.6 in) to 150 cm (59 in).

MEDICAL CONTRAINDICATIONS

GENERAL PRECAUTIONS

PulmoVista 500 should not be used in patients where the application of the electrode belt may pose a risk to the patients, e.g. patients with unstable spinal lesions or fractures.
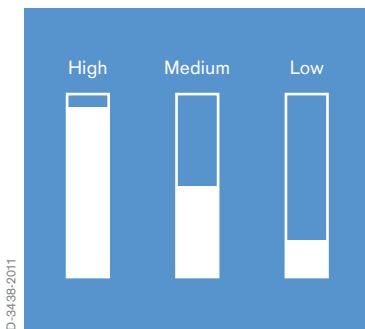
LOW SIGNAL QUALITY

Certain, extremely rare patient conditions, such as massive lung and / or tissue edema can lead to compromised signal quality. When the signal quality indicator reads "Low" and even applying electrode gel or reducing the frame rate do not lead to an improvement then PulmoVista 500 should not be used in such patients.

Similar precautions apply to obese patients. In patients with a BMI over 50 PulmoVista 500 should not be used. The signal quality of obese patients with a BMI less than 50 should be monitored closely.

EIT measurements are generally relatively sensitive to body movements. For example, lifting up the arms will cause the skin over the thorax to shift; a subsequent shift of the belt will also occur, while the position of the lung tissue remains almost unchanged. The resulting change in position of the electrodes relative to the lung tissue will induce impedance changes which are much larger than those related to ventilation.

Taking this into account, PulmoVista 500 is not suitable for ambulatory patients and patients with uncontrolled body movements.

As sufficient signal quality requires that all electrodes have proper skin contact the electrode belt must not be placed over wound dressings and the like.

ACTIVE IMPLANTS
So far, little experience exists regarding the interference between active implants and impedance tomography measurements.

For this reason, PulmoVista 500 must not be used on patients with a cardiac pacemaker, an implantable cardioverter-defibrillator (ICD) or any other active implants where the function of PulmoVista 500, especially the alternating current application, may interfere with the function of the active medical device.

In the future, compatibility tests should be performed to identify those devices where interference is likely. In case of any doubt about the compatibility with an implanted active device the PulmoVista 500 must not be used.

DEFIBRILLATION

PulmoVista 500 must not be used during cardiac defibrillation as the energy needed for defibrillation may disperse into the PulmoVista 500 and decrease the effectiveness of defibrillation.

There is also a risk of damage to the components of the PulmoVista 500 if the patient belt remains connected to the patient during defibrillation, and the electrode belt may mechanically interfere with the correct positioning of the defibrillation electrodes or paddles.

Consequently, before defibrillation is carried out the lateral patient cable connectors should be removed from the patient cable ports and the electrode belt opened.

SKIN CONDITIONS

In contrast to ECG measurements, electrodes must be also placed in the posterior region of the thorax. As the belt is positioned around the thorax the body weight of the patient is always on part of the electrode belt, regardless whether the patient is in a supine, lateral or prone position.

The silicone belt has a cushioning effect and no lesions, as a result of the patient laying on the belt, patient cable or its snaps, have been observed. Shallow indentations and skin redness have been observed at the position of the edge of the silicone belt when it has been in place for some time. These marks are similar to those caused by a crease in a bed sheet. The time taken for these marks to dissipate depends on the skin condition of the individual as well as the tightness of the belt.

In contrast to creases the EIT belt will remain in exactly the same position for the duration of the measurement period. Thus, prolonged measurement times may increase the risk of skin injury. Therefore the maximum allowable time for the belt to be in place is 24 hours - during this time the skin in the area of the electrode belt must be checked regularly. Special care needs to be taken in patients whose peripheral / skin perfusion is compromised, e.g. septic shock or other severe cardiovascular compromise.

The electrode belt of PulmoVista 500 must not be placed over injured, inflamed or otherwise damaged skin areas.

INTERFERENCE FROM OTHER MEDICAL DEVICES

To date, little experience exists regarding interference of EIT measurements with other electromedical devices and particular other bioimpedance measurements.

This includes non-invasive cardiac output monitors which use bioimpedance measurements, respiration monitors using impedance measurements, instruments for electrocautery and electrosurgery and devices designed for electricity-based therapy.

PulmoVista 500 is not intended for use in the presence of strong magnetic fields, e.g., MRI, as PulmoVista 500 or the respective device may be damaged.

8. Considerations for EIT data interpretation

SPATIAL RESOLUTION

PulmoVista 500 uses 16 electrodes to measure the voltages that are used for image reconstruction. There is a distance of approximately 3 cm between the electrodes of a large size belt (for chest circumferences between 92 cm and 110 cm). Mathematical simulations based on this electrode arrangement demonstrate a spatial resolution of 15% of the thoracic diameter, however the resolution decreases to 20% towards the center of the body.

While CT scanners typically provide images consisting of 512 x 512 pixels, EIT images from PulmoVista 500 only consist of 32 x 32 pixels, which are 256 times less pixels compared to CT images. Even though the first CT scanner, developed in 1970, only provided an array of 80 x 80 pixels, it is not expected, that the spatial resolution of EIT images can be improved in the near future to a point comparable with that of CT.

As current pathways do not lead straight through the body (unlike X-rays) and can easily change directions to bypass non-conductive regions, e.g. a pneumothorax, it is assumed that the drawbacks of an increased number of electrodes, such as additional cables and connections, a lower signal strength, higher crosstalk, will outweigh the potential benefits of a slight increase in spatial resolution.

In contrast to CT and MRI, the intended role of EIT in clinical practice is to guide ventilation therapy rather than the absolute diagnosis; it is unlikely that increased spatial resolution would significantly improve the ability of EIT to guide ventilation therapy.

ONE SINGLE CROSS-SECTIONAL PLANE

PulmoVista 500 displays EIT status images and related information which represent only the distribution of the tidal volume in one single cross-sectional plane.

As previously described it can be assumed that, due to the three dimensional current flow, the area at the center of the thorax which is reflected by EIT data is several centimeters thick; this thickness decreases towards the surface near the electrodes, resulting in a lens-shaped sample volume.

The mapping of complex three-dimensional morphological structures on a two-dimensional template further decreases spatial resolution. Additionally, there is no precise information about the size of the portion of the lungs represented by an EIT image.

When interpreting EIT data, it must be accepted that, as a result of the conditions explained above, the displayed circumference of the electrode plane does not exactly match the geometry of the patient. It also must be taken into account that the displayed position of impedance changes does not always exactly match the position where the impedance changes occur.

Physiological changes, such as increased intra-abdominal pressure, or changes in ventilator settings like the PEEP, may cause caudal-cranial shifts of intra-thoracic structures.

Those shifts have to be considered when relating tidal volumes to tidal variations or changes of EELV to ΔEELI.

Since tidal volume reflects the volume of the entire lung while tidal variations represent only the volume within the electrode plane, the assumption of a linear relationship between changes in global tidal impedance and tidal volume cannot be used to directly calculate the EELV [38].

As major changes in PEEP can alter the portion of the lung tissue which is captured by the electrode plane EIT measurement, and as recruitment and derecruitment is not necessarily evenly distributed in a caudal/cranial orientation, the strong correlation of volume changes within the electrode plane and FRC changes reflecting the entire lung, that were previously described by Hinz et al. [39] and Odenstedt et al. [28], is not seen under all clinical circumstances.

Thus, when interpreting the ΔEELI, the fact that this information only reflects changes of end-expiratory lung impedance of one slice of the lung (the electrode plane), as opposed to the entire lung, must be taken into account.

While this lack of correlation could be mistaken as a general limitation of EIT, it only confirms that EIT focuses on the juxta-diaphragmatic lung regions (assuming that the electrode belt is placed as recommended), where atelectasis, tidal and alveolar recruitment typically occur. By providing continuous information about this particular part of the lungs, the dynamics of ongoing recruitment or de-recruitment, e.g. after changes in PEEP, can be visualized [40]. Also, with its regional information on end-expiratory lung impedance changes PulmoVista 500 is the only bedside tool which enables assessment of whether such an increase was caused by hyperinflation (in the ventral regions) or the reopening of atelectatic lung tissue (in the dorsal regions).

When a global FRC parameter is used regional atelectasis could be masked by increased compliance in other regions during deflation [41]. Hickling [42] has described, in the context of the interpretation of global pressure-volume curves, that recruitment of lung regions and hyperinflation of other lung region is likely to happen simultaneously in the lungs of ARDS patients.

D-28332-2009

Fig. 40: Recommended position of the electrode belt

BELT POSITION

In an experimental study, Reske [43] assessed the correlation between non-aerated lung volume and total lung volume and PaO_2, first using a small number of representative CT slices from different planes rather then 21 CT slices representing the entire lung. It was found that one single juxta-diaphragmatic cross-section reflects the condition of the (atelectatic) lungs better than the conventional combination of apical, hiliar and juxta-diaphragmatic slices. It is known that anesthesia-induced atelectasis occurs predominantly in dependent juxta-diaphragmatic lung regions which may account for the superior performance of one single juxta-diaphragmatic slice when assessing atelectasis.

Thus it can be seen that selecting a single plane in the appropriate position – as done with EIT – may provide the best possible representation of those juxta-diaphragmatic lung regions which are most affected by atelectasis, tidal recruitment and overdistension. It is recommended to position the belt at the corresponding position between the 4th and 6th intercostal space at the mid-clavicular line.

A small number of EIT research groups continue to work on prototypes of three dimensional EIT imaging devices. However, it is not expected that these systems will be developed beyond the research setting within the next decade.

CARDIOPULMONARY INTERACTION

The impedance changes measured by PulmoVista 500 reflect an interaction of different physiological processes rather than the effects of a single, isolated phenomenon. In some publications and review papers, this is perceived as a limitation.

This point of view does not take into account that impedance changes due to ventilation are a normally about 10 times greater than impedance changes due to cardiac activity. Also, cardiac related impedance changes can quite easily be isolated using low-pass filtering.

D-65-2011
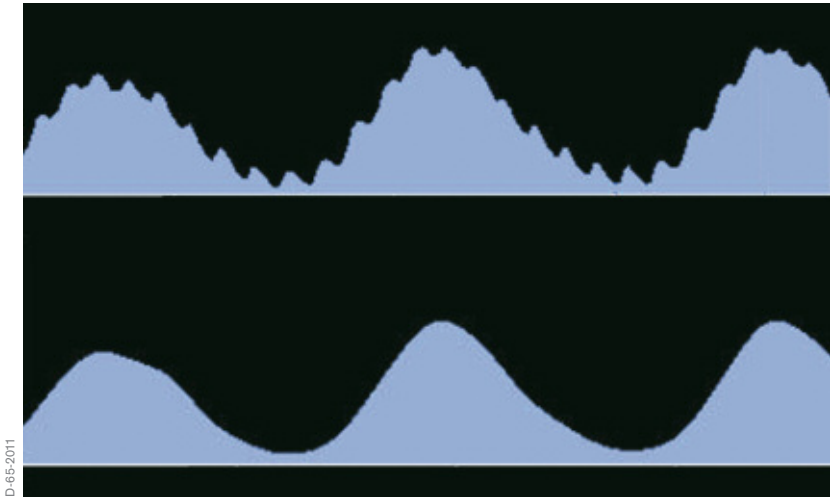
Fig. 41: Unfiltered impedance waveform (upper curve) and filtered waveform
(Cut-off frequency 35 [1/min]) from the same EIT data file

As PulmoVista 500 incorporates low pass filtering thus the concurrent
presence of impedance signals due to ventilation and cardiac activity does
not limit the assessment of regional ventilation distribution and changes of
end-expiratory lung impedance (Fig. 41).

To completely isolate impedance changes due to cardiac activity and lung
perfusion is more challenging but EIT systems have been sufficiently
improved so that very small impedance changes can be detected.
Consequently, various research groups are developing protocols to validate
the suitability of EIT for displaying cardiac images, lung perfusion images
and derived parameters which reflect aspects such as changes in stroke
volume and the regional distribution of lung perfusion. Early results look
promising for the use of EIT to monitor cardiac activity and lung perfusion.
However, further research and clinical validation must be performed before
this new functionality can be introduced into clinical practice.

ARTIFACTS

PulmoVista 500 was designed to continuously display ventilation related changes of air content within the electrode plane, however, as with many medical imaging systems, changes in the body position and movement may cause significant artifacts.

Just as moving an ultrasound probe to a different part of the body may change the ultrasound image so may changing the position of the electrode belt cause changes in the distribution of ventilation displayed by EIT; end-expiratory lung impedance values are particularly affected by changes in belt position.

Additionally, changes in position of the electrode belt, or the application of electrode gel, may alter the skin-electrode resistance and thus the EIT data so that the interpretation of the trend data provided by PulmoVista 500 may be compromised. This means that the changes, such as caused by moving the belt, must be taken into consideration when analyzing trend data.

End-expiratory lung impedance is also affected by changes of extravascular lung water content, but in contrast to belt repositioning, changes of extravascular lung water content are relatively slow and tend not to have a significant impact on the trended end-expiratory lung impedance information as the time scale of the ΔEELI trend screen is limited to 20 minutes.

It has occasionally been reported that strong electromagnetic fields in the range of the operating frequency of the EIT device have caused major artifacts in EIT data. These electromagnetic fields may exert their effect via the pathway of the patient, the mains power supply, the trunk cable or the patient cable.
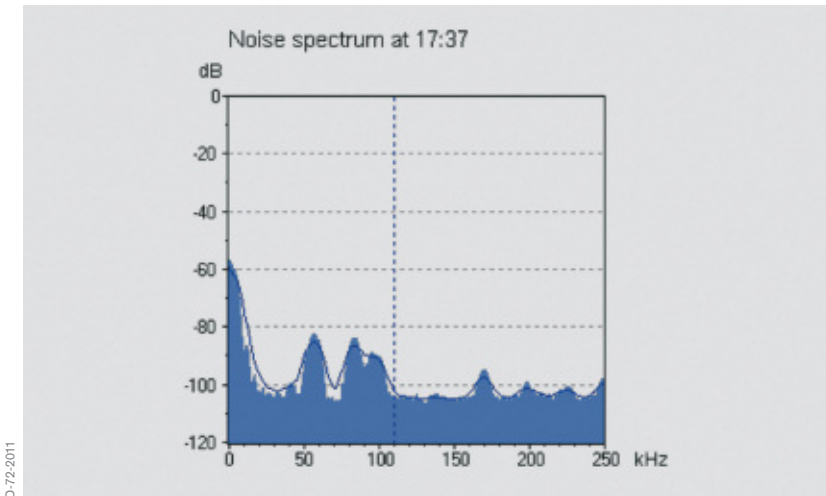
Fig. 42: Graphical display of the noise spectrum determined by PulmoVista 500 during the last calibration

Electromagnetic interference is usually limited to particular frequency bands. PulmoVista 500 prevents superposition of this kind of noise on EIT signals by analyzing the relevant spectrum of electromagnetic background noise during the calibration cycle and automatically setting the operating frequency to a range with a low background noise level. It is this feature of PulmoVista 500 which makes it less sensitive to interference from electromagnetic fields than previous generations of EIT devices.

RELATIVE IMPEDANCE CHANGES

Until now, most of the relevant studies were performed using functional EIT (f-EIT), which measures impedance changes relative to a baseline. Absolute EIT (a-EIT) may also become clinically useful, as being able to measure absolute regional impedance values would allow one to directly distinguish between lung conditions which result from regions with lower

resistivity (e.g. hemothorax, pleural effusion, atelectasis and lung edema) and those with higher resistivity (e.g. pneumothorax, emphysema).

However, the reconstruction of absolute impedance images requires that the exact dimensions and the shape of the body, as well as the precise location of the electrodes, be taken into account, as simplified assumptions would lead to major reconstruction artifacts.

While initial studies assessing aspects of a-EIT have already been published [44], as of today this area of research has not yet reached the level of maturity which would make it suitable for clinical use. Consequently, PulmoVista 500 does currently not provide a-EIT functionality.

9. Validation studies

Electrical impedance tomography has been extensively validated in animal experiments and clinical (human) studies. In animal experiments the spatial distribution of pulmonary aeration determined by EIT is well correlated with results from CT, single photon emission CT (SPECT) and electron beam CT (EBCT). These findings were obtained using different EIT devices, diverse ventilator modes and settings.

Notably a strong correlation between EIT and CT was demonstrated in critically ill patients.

ANIMAL STUDIES

Lüpschen et al. compared EIT to CT in 10 domestic pigs undergoing laparoscopic surgery and pulmonary lavage [45]. They found that the EIT images exhibited a good spatial correlation with the CT reference images. The high temporal resolution of EIT means that effects of changed ventilator settings can be seen immediately. Functional activity and tidal variation show an excellent linear correlation with tidal volume (i.e. global ventilation), which indicates that information on regional ventilation may be gained from EIT images and/or local impedance changes.

Hinz et al. validated EIT for the measurement of regional distribution of ventilation by comparing it to single photon emission CT (SPECT) [46]. They investigated in twelve pigs, whether regional impedance changes obtained by EIT are quantitatively related to regional ventilation as determined by SPECT. Different modes of mechanical and spontaneous ventilation were analyzed in this study. A highly significant linear correlation between regional ventilation measured by EIT and SPECT scanning was found ($R^2 = 0.92$; range 0.86 to 0. 97).

The mode of ventilation, or presence of spontaneous breathing, did not affect the correlation in a significant manner. Moreover, induced lung injury, induced changes of compliance of the respiratory system or of extravascular lung water content caused no significant effects on the correlation between EIT and SPECT.

Frerichs et al. validated the ability of EIT to detect local changes in air content resulting from modified ventilator settings by comparing data from EIT with data from Electron Beam CT (EBCT), obtained under identical steady state conditions [47]. The experiments were carried out in six pigs using five different tidal volumes at three PEEP levels. The analysis was performed in six regions of interest, located in the ventral, middle and dorsal areas of each lung. Good correlation between the changes in lung air content determined by EIT and EBCT was revealed, with mean correlation coefficients in the ventral, middle and dorsal regions of 0.81, 0.87 and 0.93 respectively.

Frerichs et al. investigated the reproducibility of EIT images showing lung ventilation distribution at different PEEP levels in 10 pigs [48]. Regional lung ventilation was determined in the right and left hemithorax as well as in 64 regions of interest evenly distributed over each side of the chest in the ventro-dorsal direction. Ventilation distribution in both lungs was visualized as ventro-dorsal ventilation profiles and shifts in ventilation distribution quantified in terms of centres of ventilation in relation to the chest diameter. The proportion of the right lung on total ventilation in the chest cross-section was 0.54 ± 0.04 and remained unaffected by repetitive PEEP changes. In summary, the authors found excellent reproducibility of the results in individual regions of interest with almost identical patterns of ventilation distribution during repeated PEEP changes.

Van Gendringen et al. investigated the value of EIT for the assessment of regional lung mechanics during high-frequency oscillatory ventilation (HFOV) in eight pigs [49]. Lung volume determined by EIT was estimated by

calibrated strain-gauge plethysmography (SGP) during a P-V maneuver. Regional lung volume changes were assessed by electrical impedance tomography in various regions of interest. The study showed good agreement between impedance from EIT and lung volume estimated by SGP, during both the P-V maneuver and subsequent HFOV. However, baseline measurements performed at the end of the experiments suggested that accumulation of intra-thoracic fluid may limit the accuracy for determining small changes in lung volume over a longer period of time.

Meier et al. investigated the capability of EIT to monitor regional lung recruitment and lung collapse using different levels of PEEP in a lavage model of lung injury in six domestic pigs by comparing EIT findings to simultaneously acquired CT images and global ventilation parameters [27]. They found a close correlation between end-expiratory gas volumes assessed by EIT and end-expiratory gas volumes calculated from CT (r = 0.98-0.99). Also, correlation of tidal volumes was demonstrated (r = 0.55-0.88) for both EIT and CT. The authors concluded that EIT is suitable for monitoring the dynamic effects of PEEP variations on the regional change of tidal volume, and that it is superior to global ventilation parameters in assessing the beginning of alveolar recruitment and lung collapse.

PATIENT STUDIES

Victorino et al. performed a validation study comparing EIT with dynamic CT in ten critically ill mechanically ventilated patients [50]. Their data showed that EIT reliably provides a means to assess imbalances in distribution of tidal volume in critically ill patients. When comparing regional ventilation across different thoracic regions, the quantitative information provided by EIT carries good proportionality to changes in air content as calculated by dynamic CT scanning – but not with CT gas/tissue ratio or CT mean-densities. Further results from this study showed that EIT images from patients undergoing controlled mechanical ventilation were reproducible and presented good agreement to dynamic CT scanning. Moreover, regional impedance changes in the EIT slice were best explained

by the corresponding changes in air-content detected in the CT slice (explaining 92 - 93% of its variance). Other CT derived variables, such as regional X-ray mean-density or regional gas-tissue ratio, did not parallel regional changes in impedance as consistently. It was also noted that good correlation between EIT and CT could only be observed in sufficiently large regions of interest. This finding was to be expected considering the limited spatial resolution of EIT and is in line with results from mathematical calculations.

Riedel et al. evaluated the effect of body position and positive pressure ventilation on intrapulmonary tidal volume distribution in ten healthy adult subjects [51]. EIT measurements and multiple-breath sulphur hexafluoride (SF6) washout were performed. Profiles of average relative impedance change in regional lung areas were calculated. Relative impedance time course analysis and Lissajous figure loop analysis were used to calculate phase angles between dependent or independent lung and total lung (Φ). EIT data were compared to SF6 washout data measuring the lung clearance index (LCI). Proposed EIT profiles allowed inter-individual comparison of EIT data and identified areas with reduced regional tidal volume using pressure support ventilation. The phase angle Φ of dependent lung in various body positions is as follows: supine 11.7 ±1.4, prone 5.3 ±0.5, right lateral 11.0 ±1.3 and left lateral 10.8 ±1.0. LCI increased in the supine position from 5.63 ±0.43 to 7.13 ±0.64 in the prone position. Measured Φ showed an inverse relationship to LCI in the four different body positions. The findings of this study demonstrate that functional EIT measures gravity dependent asynchronous emptying of the lung in different body positions and characterises local tidal volume distribution at different levels of pressure support. Although this study was limited to healthy subjects, and rather large lung areas were analysed, the authors state that the proposed method may be powerful enough to analyse uneven ventilation in sick lungs and more specific lung regions.

10. Examples of EIT status images

While radiological and EIT images both provide information about the regional distribution of air in the lungs the image characteristics provided by these modalities are quite different.

The difference in spatial and temporal resolution has previously been discussed.

Radiological images of the lung provide information on the air content and reflect, depending on the moment the images were taken, the end-inspiratory, the end-expiratory status or a lung condition somewhere in between.

EIT images reflect the lung function, not the lung itself, which means EIT displays ventilated lung regions rather than morphological or anatomical structures of the lung.

Nonetheless, the regional information contained in EIT and CT images is closely related to each other when pathological conditions such as pleural effusion or atelectasis lead to non-aerated and non-ventilated lung regions. While CT images display lungs regions with trapped air (e.g. pneumothorax) in black because of the large air content, EIT also displays those regions in black because they are not ventilated. Conversely a CT image may indicate a region of consolidated lung tissue in a white color because of the high fluid content, while this region might be displayed in the EIT image in black or dark blue color, if this region is not or only partially ventilated.

In this chapter, various examples of EIT status images are provided as an introduction to the world of EIT images. Where available, radiographic chest images from the same patient are shown as well.

Please note that the comparability of the displayed EIT images and the related radiographic chest images or CT images may be limited due to the fact that the images were taken at different times and there may also be some variation in the caudo-cranial aspect of the images.

All EIT images were taken in the juxta-diaphragmatic plane.

D-50-2011
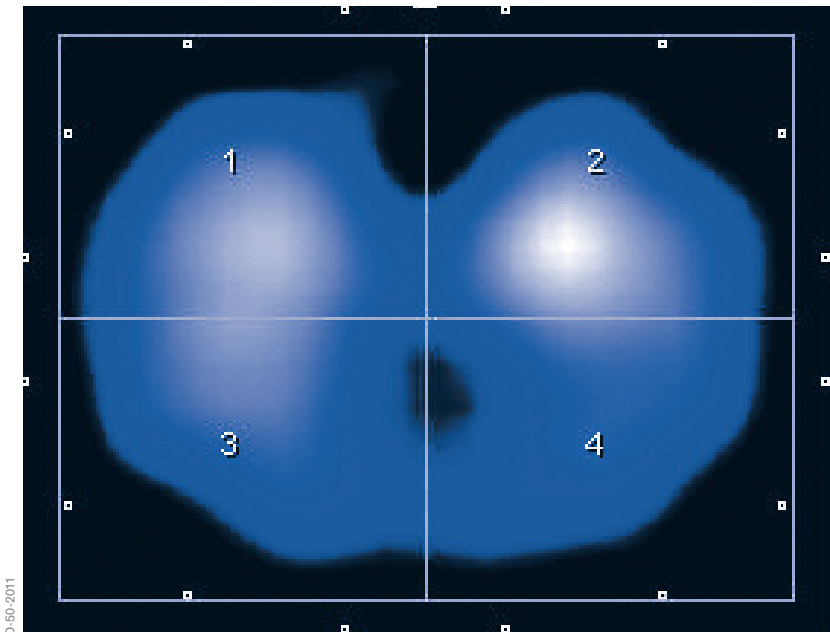
Fig. 43: Tidal image of a healthy individual

EXAMPLE 1: HEALTHY LUNG

Ventilation is quite evenly distributed over the quadrants of the image
(ROI 1 = 28 %, ROI 2 = 26 %, ROI 3 = 25 %, ROI 4 = 21 %). Typically, the right
lung (ROI 1 and ROI 3 in this ROI arrangement) receives 50 - 55 % of global
ventilation (100 %) in a sitting or supine individual, which corresponds to
findings in the literature [52]. This distribution changes significantly, even
in healthy volunteers, during lateral positioning.

Fig. 44: Tidal image of a healthy obese individual

EXAMPLE 2: HEALTHY LUNG OF AN OBESE VOLUNTEER
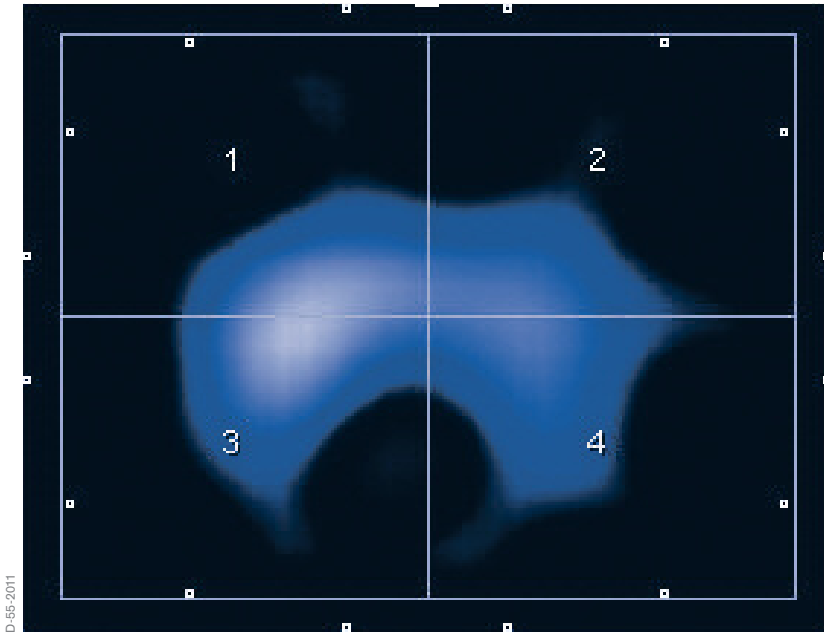In obese individuals with healthy lungs, the distribution within the quadrants does not differ significantly (ROI 1 = 24 %, ROI 2 = 20 %, ROI 3 = 29 %, ROI 4 = 26 %) from individuals with normal body weight. However, the ventilated regions appear to be much smaller, as the lungs are surrounded by a large area of fatty tissue.
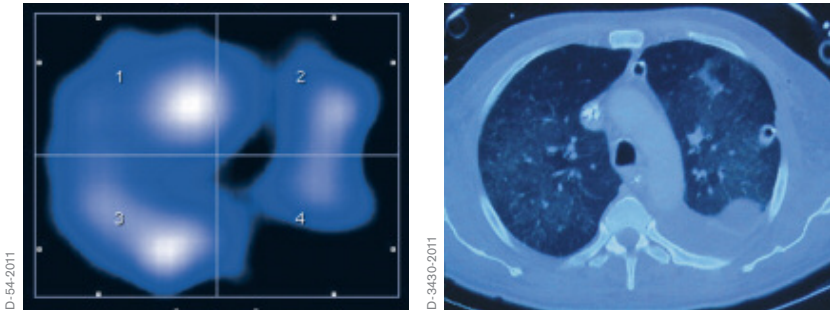
Fig. 45: Tidal image and corresponding CT image of a patient with pleural effusion in the left lung

EXAMPLE 3: PLEURAL EFFUSION

Fluid accumulation, such as a pleural effusion, represents a non-ventilated area; In the EIT image, this is displayed as a black area. On the CT image this region, due to its density, is shown as an area of higher contrast than the surrounding lung tissue.

The EIT image suggests a mediastinal displacement towards the left lung which was not visible in the CT image (taken about 5 hours earlier).

The non-ventilated area is reflected by significant reduction of regional ventilation in the lower right quadrant. The distribution of ventilation was ROI 1 = 35 %, ROI 2 = 20 %, ROI 3 = 31, ROI 4 = 14.
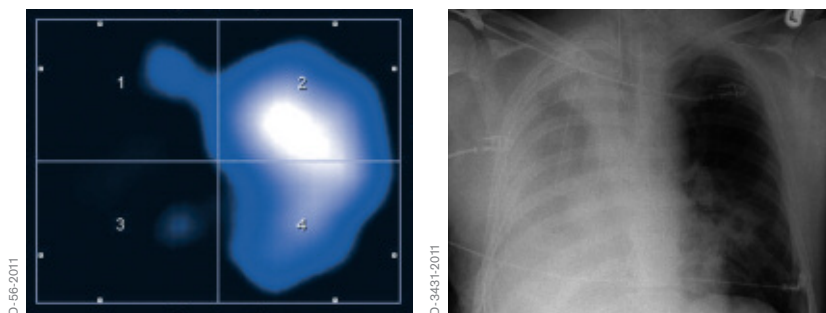
Fig. 46: Tidal image and corresponding chest X-ray of a patient with pneumectomy

EXAMPLE 4: RIGHT SIDED PNEUMONECTOMY

As there is no ventilation in the right hemithorax after a pneumonectomy the corresponding area on an EIT image (transverse plane) is black. In contrast on a chest X-ray (frontal plane) this area is white, as the right hemithorax is filled with fluid and connective tissue. The distribution of ventilation was ROI 1 = 2 %, ROI 2 = 55 %, ROI 3, = 1 %, ROI 4 = 42 %.
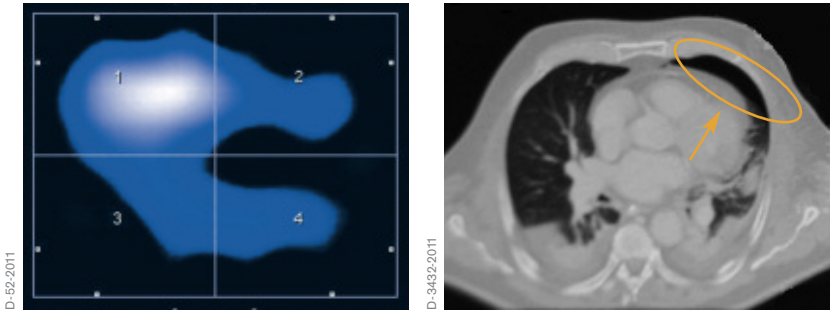
Fig. 47: Tidal image and corresponding CT image of a patient with a pneumothorax in the left lung

EXAMPLE 5: PNEUMOTHORAX

This EIT image reveals that most of the ventilation is occurring in ROI 1, the cause of the poor distribution is revealed by the more anatomically specific CT image: a pneumothorax (marked by the blue line) in the ventral region of the left lung and bilateral dorsal atelectasis and effusion.

ROI 1 is receiving 56 % of the "Tidal Variation" while, due to the pneumothorax, ROI 2 is receiving just 16 % of the global "Tidal Variation" and due to the dorsal pathology ROI's 3 and 4 are receiving just 15 and 13 % respectively.
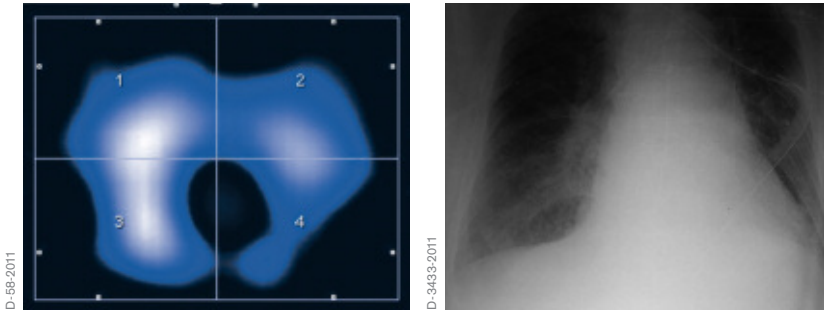
Fig. 48: Tidal image and corresponding chest X-ray of a patient with dorsal atelectasis

EXAMPLE 6: ATELECTASIS

The EIT image shows that the functional impairment of the two basal lung regions was not symmetrical even though the chest X-ray indicates bilateral atelectasis. The basal portions of the right lung, (ROI 3) still received 31 % of the global "Tidal Variation" while the corresponding area of the left lung, (ROI 4) only received 15 %.
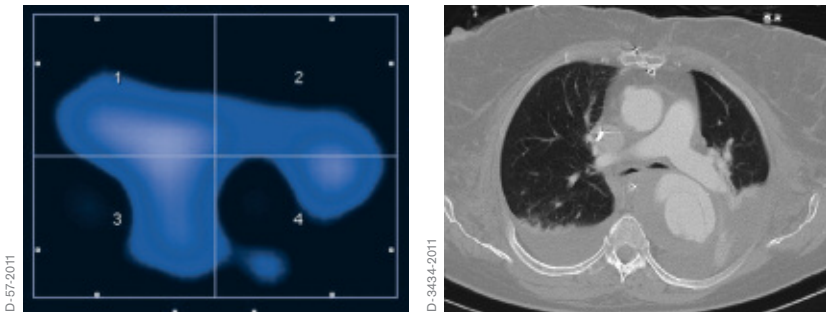
Fig. 49: Tidal image and corresponding CT image of a patient with dystelactasis

EXAMPLE 7: DYSTELECTASIS

The CT-Scan shows marked dystelectasis in the dependent (dorsal) region of the left lung with fluid accumulation, and smaller dystelectic areas in the dependent areas of the right dorsal lung. The shape of the ventilated regions as displayed in the EIT image does not match the lung regions filled with air in the CT image. However, the impaired ventilation in the left lower lobe is clearly reflected in ROI 4 of the EIT image.

"Tidal Variations" were highly unevenly distributed within ROI 1 (35 %) and ROI 2 (19 %). The lack of ventilation in the upper part of those regions suggests overdistension of the upper lung regions.

ROI 3 received 27 % of the global "Tidal Variations", while the regional "Tidal Variations" (20 %) in ROI 4 was only accessing the upper third of ROI 4, due to the dystelectasis.
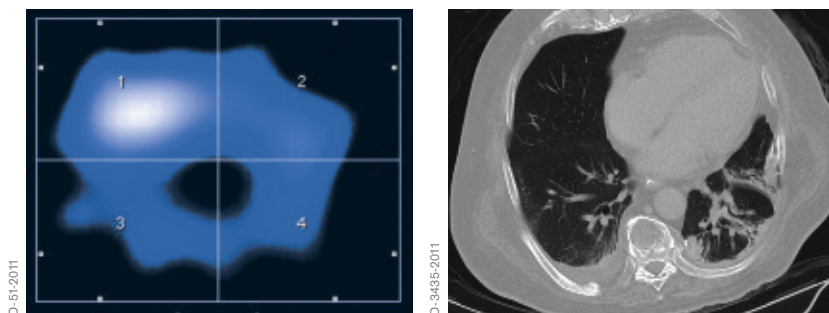
Fig. 50: Tidal image and corresponding CT image of an ARDS patient

EXAMPLE 8: ARDS

The CT scan shows a typical inhomogeneous air distribution of an ARDS patient. The dorsal parts of both lungs (left more than right) were especially impaired. In the EIT image, this inhomogeneity is reflected by reduced ventilation in both dorsal quadrants 16 % (ROI 3) and 14 % (ROI 4), while the ventral regions received 46 % (ROI 1) and 23 % (ROI 2).
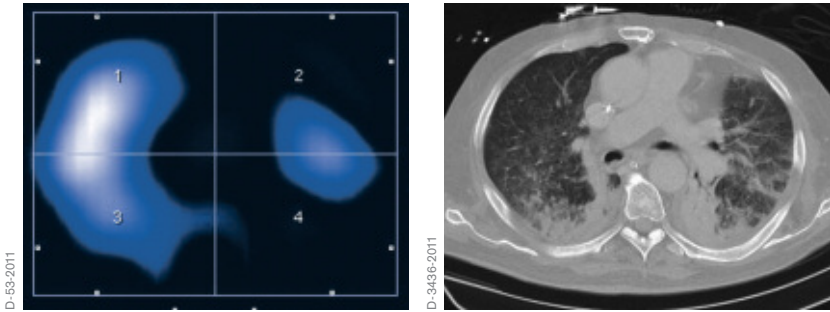
Fig. 51: Tidal image and corresponding CT image of an ARDS patient

EXAMPLE 9: ARDS

The CT scan shows the typical picture of late ARDS with diffuse infiltrates throughout nearly all lung regions. While the CT scan seems to show no major difference in the severity of alteration between both lungs, the EIT image shows a very uneven distribution of Tidal Variations. The upper right lung (ROI 1) received 46 %, the lower right lung (ROI 3) 39 %. The impedance waveforms revealed a significantly delayed filling in ROI 2 and ROI 4, leaving just 15 % of the tidal volume (ROI 2 = 5 %; ROI4 = 10 %) for the left lung. This example shows how EIT can provide additional information to other non-dynamic imaging modalities.

11. Outlook

Prior to the introduction of PulmoVista 500 all EIT devices were solely used to address research related questions, which means that at present there is limited experience about the use of this novel information provided by EIT in daily clinical practice.

It is anticipated that, initially, experts in mechanical ventilation and respiratory monitoring will rapidly develop further experience in using EIT in daily clinical practice now that PulmoVista 500 has been made available by Dräger.

At the same time however, the availability of PulmoVista 500 will likely also boost further research activities, as from now on EIT data can conveniently and reliably be collected over hours with an approved medical device.

For example, various approaches to the extraction of diagnostic information from EIT data have already been described by researchers: in the future these methods might be established as being suitable to notify the clinician about lung conditions that need to be avoided, such as overdistension or cyclic opening and closing of lung regions.

Costa et al. [53] have described an algorithm that estimates recruitable alveolar collapse and hyperdistension utilizing EIT data collected during a decremental PEEP trial. Recently Löwhagen et al. [54] developed an algorithm to assess the regional redistribution of gas throughout the inspiratory phase during a decremental PEEP trial, subsequent to a recruitment maneuver.

It becomes more and more obvious that the greatest value in the diagnostic interpretation of EIT data can be obtained when algorithms are applied during therapeutic maneuvers that induce regional redistribution of tidal

volumes and changes of end-expiratory lung volumes. It is this specific information that reveals how the lungs of the individual patient respond to different ventilation strategies.

Not surprisingly, initial approaches have already been described [41] about using EIT based diagnostic information as an input source for future expert systems which automatically adjust ventilator settings according to the requirements of the individual patient, thus continuously maintaining lung protective ventilation strategies.

Another application field receiving increasing interest within the research community is the EIT based estimation of regional distribution of pulmonary perfusion. While the approaches described so far [55, 56, 57] certainly need further validation, such supplementary information would be of even greater clinical value to the physician, as for the first time, not only the distribution of ventilation but also the regional ventilation/perfusion ratio could be determined non-invasively and continuously at the bedside.

In the research setup, early EIT devices have also been used with promising results to assess the amount of extravascular lung water [58], thus providing means to monitor lung edema. The latest experiments in this field [59, 60] utilized impedance spectroscopy where –in contrast to EIT- the frequency of the applied alternating current varies over a broad band. The generation of spectral information allows a classification or separation of different tissue types, a method, which is also utilized by conventional body composition monitors.

In conclusion, even after 30 years of research the field of EIT remains broad and wide open for further enhancements and new applications. The market introduction of PulmoVista 500 is clearly a significant milestone in the long history of EIT.

Appendix I: Literature references

1 Gattinoni L, Pesenti A, Bombino M, Baglioni S, Rivolta M, Rossi F, Rossi G, Fumagalli R, Marcolin M, Mascheroni D, Torresin A. Relationships between lung computed tomographic densitiy, gas exchange, and PEEP in Acute Respiratory Failure. Anesthesiology 1988; 69: 824-832

2 Slutsky AS, Tremblay LN. Multiple system organ failure. Is mechanical ventilation a contributing factor? Am J Respir Crit Care Med 1998; 157: 1721-1725

3 Simon BA, Easley RB, Grigoryev DN et al. Microarray analysis of regional cellular responses to local mechanical stress in acute lung injury. Am J Physiol Lung Cell Mol Physiol 2006; 291: L851-L86

4 Ranieri VM, Suter PM, Tortorella C, et al. Effect of mechanical ventilation on inflammatory mediators in patients with acute respiratory distress syndrome—A randomized controlled trial. JAMA 1999; 282: 54-61

5 Gentile MA, Cheifetz IM. Optimal positive end-expiratory pressure: The search for the Holy Grail continues. Crit Care Med 2004; 32: 2553-2554

6 Markhorst D, Kneyber M, van Heerde M. The quest for optimal positive endexpiratory pressure continues. Crit Care 2008; 12: 408

7 Crotti S, Mascheroni D, Caironi P et al. Recruitment and derecruitment during acute respiratory failure: a clinical study. Am J Respir Crit Care Med 2001; 164: 131-140

8 Pelosi P, Goldner M, McKibben A et al. Recruitment and derecruitment during acute respiratory failure: an experimental study. Am J Respir Crit Care Med 2001; 164: 122-130

9 Kunst PW, Vazquez de Anda G, Bohm SH, Faes TJ, Lachmann B, Postmus PE, de Vries PM. Monitoring of recruitment and derecruitment by electrical impedance tomography in a model of acute lung injury. Crit Care Med 2000; 28: 3891-3895

10 Kunst PW, Bohm SH, Vazquez de Anda G, Amato MB, Lachmann B, Postmus PE, de Vries PM. Regional pressure volume curves by electrical impedance tomography in a model of acute lung injury. Crit Care Med 2000; 28: 178-183

11 Genderingen HR, Vught AJ, Jamsen JRC. Estimation of regional volume changes by electrical impedance tomography during a pressure-volume maneuver. Intensive Care Med 2003; 29: 233-240

12 Holder, D. S., Clinical and physiological applications of Electrical Impedance Tomography. UCL Press 1993; ISBN 1-85728-164-0 HB

13 Holder, D. S., Electrical Impedance Tomography Methods, History and Applications. IOP 2005; ISBN 0 7503 0952 0

14 Arnold JH Electrical impedance tomography: On the path to the Holy Grail. Crit Care Med 2004; 32: 894-895

15 Hinz J, Hahn G, Quintel M, Elektrische Impedanztomographie - Reif für die klinische Routine bei beatmeten Patienten? Anaesthesist 2008; 57: 61-69

16 Barber DC, Brown BH. Recent developments in applied potential tomography-APT. In: Proceedings of 9th Conference on Information Processing in Medical Imaging. Ed. S.L. Bacharach, Martinus Nijhoff, Dordrecht 1986; pp. 106-121

17   Yorkey TJ, Webster JG, Tompkins WJ. Comparing Reconstruction
     Algorithms for Electrical Impedance Tomography. IEEE Trans.
     On Biomedical Engineering 1987; vol 34, no. 11, pp. 843-852

18   Faes TJ, Meij HA van der, Munck JC de, Heethaar RM. The electric
     resistivity of human tissues (100 Hz–10 MHz): a meta-analysis of review
     studies. Physiol Meas 1999; 20: R1-10

19   Barber DC. A review of image reconstruction techniques for electrical
     impedance tomography. Med Phys 1989; 16 (2): 162-169

20   Visser KR. Electric properties of flowing blood and impedance
     cardiography. AnnBiomed Eng 1989; 17: 463-473

21   Brenner D, Elliston C, Hall E, Berdon W. Estimated risks of radiation-
     induced fatal cancer from pediatric CT. AJR Am J Roentgenol 2001; 176:
     289-296

22   Brenner DJ, Hall EJ. Computed tomography–an increasing source of
     radiation exposure. N Engl J Med 2007; 357: 2277-2284

23   Wrigge H. et al. Electrical impedance tomography compared with thoracic
     computed tomography during a slow inflation maneuver in experimental
     models of lung injury. Crit Care Med 2008; Vol. 36, No. 3, p1-7

24   Erlandson K et al. Positive end-expiratory pressure optimization using
     electric impedance tomography in morbidly obese patients during laparo-
     scopic gastric bypass surgery. Acta Anaesthesiol Scand 2006; 50: 833-839

25   Hinz J, Gehoff A, Moerer O, Frerichs I, Hahn G, Hellige G, Quintel M.
     Regional filling characteristics of the lungs in mechanically ventilated
     patients with acute lung injury. Eur J Anaesthesiol 2007; 24: 414-424

26 Muders T, Luepschen H, Putensen C. Regional Ventilation Delay Index: Detection of Tidal Recruitment using Electrical Impedance Tomography. Yearbook of Intensive Care and Emergency Care 2009; 405-412

27 Meier T, Luepschen H, Karsten J, Leibecke T, Großherr M, Gehring H, Leonhardt S. Assessment of regional lung recruitment and derecruitment during a PEEP trial based on electrical impedance tomography. Intensive Care Med 2008; 34: 543-550

28 Odenstedt et al. Slow moderate pressure recruitment maneuver minimizes negative circulatory and lung mechanic side effects: evaluation of recruitment maneuvers using electric impedance tomography, Intensive Care Med 2005; 31: 1706-1714

29 Frerichs I. et al. Topographic distribution of lung ventilation in artificially ventilated babies. In: Heart and Lung Assistance (Lecture Notes of the ICB Seminars), Eds. Z. Religa, Z. Rondio, G. Ferrari, M. Darowski; International Centre of Biocybernetics, Warsaw, 2000; 115-121

30 Putensen C. Electrical impedance tomography guided ventilation therapy. Current Opinion in Critical Care 2007; 13: 344-350

31 Lindgren S. Regional lung derecruitment after endotracheal suction during volume- or pressure-controlled ventilation: a study using electric impedance tomography. Intensive Care Med 2007; 33: 172-180

32 Lindgren S et al. Bronchoscopic suctioning may cause lung collapse: a lung model and clinical evaluation. Acta Anaesthesiol Scand. 2008; 52: 209-218

33 Alsaghir AH, Martin CM. Effect of prone positioning in patients with acute respiratory distress syndrome: a meta-analysis. Crit Care Med 2008; 36: 603-609

34 Sud S, Sud M, Friedrich JO, Adhikari NK. Effect of mechanical ventilation in the prone position on clinical outcomes in patients with acute hypoxemic respiratory failure: a systematic review and meta-analysis. CMAJ 2008; 178: 1153-1161

35 Heinrich S, Schiffmann H, Frerichs A, Klockgether-Radke A, Frerichs I. Body and head position effects on regional lung ventilation in infants: An electrical impedance tomography study. Intensive Care Med 2006; 32: 1392-1398

36 Bein T, Ploner F, Ritzka M, Pfeifer M, Schlitt HJ, Graf BM. No change in the regional distribution of tidal volume during lateral posture in mechanically ventilated patients assessed by electrical impedance tomography. Clin Physiol Funct Imaging 2010; Vol 30 Issue 4; 234-240

37 Steinmann D. Electrical impedance tomography to confirm correct placement of double-lumen tube: a feasibility study, British Journal of Anaesthesia 2008; 101(3): 411-418

38 Bikker IG et al. Lung volume calculated from electrical impedance tomography in ICU patients at different PEEP levels. Intensive Care Med. 2009 Aug; 35(8): 1362-7. Epub 2009 Jun 10

39 Hinz et al. End-expiratory lung impedance change enables bedside monitoring of end-expiratory lung volume change, Intensive Care Med 2003; 29:37–43

40 Bikker IG, Leonhardt S, Miranda DR, Bakker J, Gommers D. Bedside measurement of changes in lung impedance to monitor alveolar ventilation in dependent and non-dependent parts by electrical impedance tomography during a positive end-expiratory pressure trial in mechanically ventilated intensive care unit patients, Critical Care 2010; 14: R100 1-9

41 Lüpschen H, Meier T, Grossherr M, Leibecke T, Karsten J, Leonhardt S. Protective ventilation using electrical impedance tomography, Physiol Meas 2007; 28: S247-S260

42 Hickling KG. Reinterpreting the pressure-volume curve in patients with acute respiratory distress syndrome, Current Opinion in Critical Care 2002; Vol 8-1, 32-38

43 Reske AW. Analysis of the nonaerated lung volume in combinations of single computed tomography slices – is extrapolation to the entire lung feasible? Critical Care Volume 11 Suppl 2, 27th International Symposium on Intensive Care and Emergency Medicine 2007; P206, p.85

44 Hahn G. et al. Imaging pathologic pulmonary air and fluid accumulation by functional and absolute EIT. Physiol. Meas. 2006; 27 1-12

45 Luepschen H et al. Clinical applications of thoracic electrical impedance tomography. 6th conference on biomedical applications of electrical impedance tomography, London, June 22-24, 2005

46 Hinz J, Neumann P, Dudykevych T, Andersson LG, Wrigge H, Burchardi H, Hedenstierna G. Regional Ventilation by Electrical Impedance Tomography: A Comparison With Ventilation Scintigraphy in Pigs, Chest 2003; 124: 314-32

47 Frerichs I, Hinz J, Herrmann P, Weisser G, Hahn G, Dudykevych T, Quintel M, Hellige G. Detection of local lung air content by electrical impedance tomography compared with electron beam CT, J Appl Physiol 2002; 93: 660-666

48 Frerichs I, Schmitz G, Pulletz S, Schädler D, Zick G, Scholz J, Weiler N. Reproducibility of regional lung ventilation distribution determined by electrical impedance tomography during mechanical ventilation. Physiol Meas 2007; 28: S261-267

49 Genderingen HR, Vught AJ, Jamsen JRC. Estimation of regional volume changes by electrical impedance tomography during a pressure-volume maneuver. Intensive Care Med 2003; 29: 233-240

50 Victorino JA, Borges JB, Okamoto VN, Matos GF, Tucci MR, Caramez MP, Tanaka H, Sipmann FS, Santos DC, Barbas CS, Carvalho CR, Amato MB. Imbalances in regional lung ventilation: a validation study on electrical impedance tomography. Am J Respir Crit Care Med 2004;169: 791-800

51 Riedel T, Richards T, Schibler A. The value of electrical impedance tomography in assessing the effect of body position and positive airway pressures on regional lung ventilation in spontaneous breathing subjects, Intensive Care Med 2005; 31: 1522-1528

52 Pierre A. F., Pneumonectomy: historical perspective and prospective insight, Eur J Cardiothorac Surg 2003; 23:439-445

53 Costa ELV et al. Bedside estimation of recruitable alveolar collapse and hyperdistension by electrical impedance tomography, Intensive Care Med 2009; 35:1132-1137

54 Löwhagen K, Lundin S, Stenqvist O. Regional intratidal gas distribution in acute lung injury and acute respiratory distress syndrome, Minerva Anestesiol 2010; 76 (12): 1024-1035

55 Fagerberg A, Stenqvist O, Åneman A. Monitoring pulmonary perfusion by electrical impedance tomography: an evaluation in a pig model, Acta Anaesthesiol Scand 2009; 53: 152-158

56 Smit HJ et al. Electrical impedance tomography to measure pulmonary perfusion: is the reproducibility high enough for clinical practice? Physiol. Meas. 2003; 24: 491-499

57 Deibele JM, Lüpschen H, Leonhardt S. Dynamic separation of pulmonary and cardiac changes in electrical impedance tomography, Physiol. Meas. 2008; 29: S1–S14

58 Kunst PWA et al. Electrical Impedance Tomography in the Assessment of Extravascular Lung Water in Noncardiogenic Acute Respiratory Failure, CHEST 1999; 116: 1695-1702

59 Mayer M, Brunner P, Merwa R, et al. Direct reconstruction of tissue parameters from differential multifrequency EIT in vivo, Physiol Meas 2006; 27: S93–S101

60 Beckmann L, Cordes A, Saygili E, Schmeink A, Schauerte P, Walter M, Leonhardt S. Monitoring of body fluid in patients with chronic heart failure using Bioimpedance-Spectroscopy. World Congress on Medical Physics and Biomedical Engineering 2009; Munich; Sep. 7-12

61 Bodenstein M, David M, Markstaller K. Principles of electrical impedance tomography and its clinical application, Crit Care Med 2009; Vol. 37, No. 2, p. 1-12

62 Geddes LA, Baker LE. The specific resistance of biological material – a compendium of data for the biomedical engineer and physiologist. Med Biol Eng 1967; 5: 271–293

63 Heyward VH. Practical body composition assessment for children, adults, and older adults. Int J Sport Nutr 1998; 8: 285–307

64 Nopp P, Rapp E, Pfützner H, Nakesch H, Ruhsam Ch. Dielectric properties of lung tissue as a function of air content, Phys. Med. Biol. 38 1993; p. 699-716

65 Nopp P, Harris ND, Zhao TX, Brown BH. Model for the dielectric properties of human lung tissue against frequency and air content. Med. & Biol. Engin. & Computing 1997; p 695-702

66 Bernard GR, Artigas A, Brigham KL, Carlet J, Falke K, Hudson L, Lamy M, Legall JR, Morris A, Spragg R., The American-European Consensus Conference on ARDS. Definitions, mechanisms, relevant outcomes, and clinical trial coordination; Am J Respir Crit Care Med. 1994 Mar;149(3 Pt 1):818-24.

Appendix II: Determining the biological impedance of the lung

Before the term bioimpedance can be fully understood, the basic understanding of electrical impedance is necessary.

DEFINITION OF ELECTRICAL IMPEDANCE
Electrical impedance, or simply impedance, describes a measure of opposition of a material to a sinusoidal alternating current (AC).

Electrical impedance extends the concept of resistance R described by Ohm's law (V=I*R) to AC circuits. Impedance describes not only the relative amplitudes of the voltage V and current I, but also their relative phases.

As both capacitors and inductors cause either negative or positive phase shifts between voltage and current, the term impedance is generally applied when electrical AC circuits contain capacitive and/or inductive elements.

HOW TO EXPRESS IMPEDANCE
Mathematically, electrical impedance $\tilde{Z}$ describes a complex number: it consists of a real and an imaginary component. Dimensionally, impedance is the same as resistance; the SI unit is the Ohm (Ω) for both entities.

There are two ways to express impedance mathematically:

Polar Form: $$\tilde{Z} = Ze^{j\theta}$$

The polar form conveniently captures both magnitude and phase characteristics, where the magnitude Z represents the ratio of the amplitude of the voltage difference to the current amplitude, while the argument θ gives the phase difference between voltage and current and j is the imaginary unit.

Cartesian Form: $\tilde{Z} = R + jX$

In the Cartesian representation, the real part of impedance is the resistance R and the imaginary component is the reactance X.
In the literature, the graph displayed in fig. 52 is often used to illustrate the relationship between resistance R, reactance X and impedance $\tilde{Z}$.
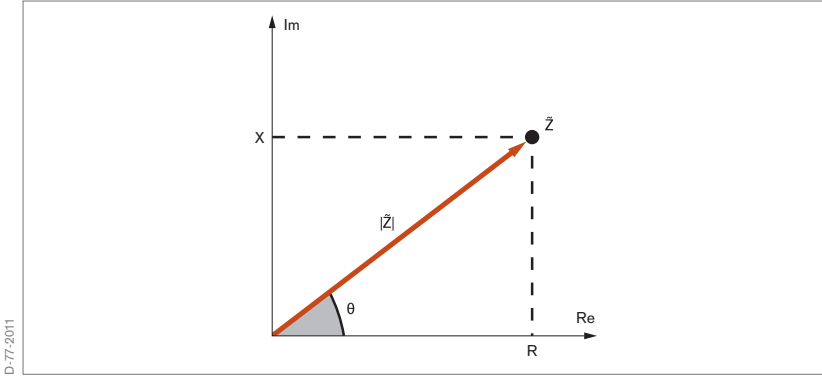
Fig. 52: Relationship between R, reactance X and impedance $\tilde{Z}$

The impedance of an ideal resistor is purely real and is referred to as a resistive impedance

$$\tilde{Z}_R = R$$

Ideal inductors L and capacitors C have a purely imaginary reactive impedance.

$$\tilde{Z}_L = j\omega L \qquad \tilde{Z}_C = \frac{1}{j\omega C}$$

The term ω equals $2\pi f$. This means that the impedance of an inductor and a capacitor, and thus the electrical behavior of inductive or capacitive AC circuits, is a function of the frequency of the applied alternating current. Thus, the impedance expresses the effects of those AC circuits or materials on phase shifts between voltage and current.
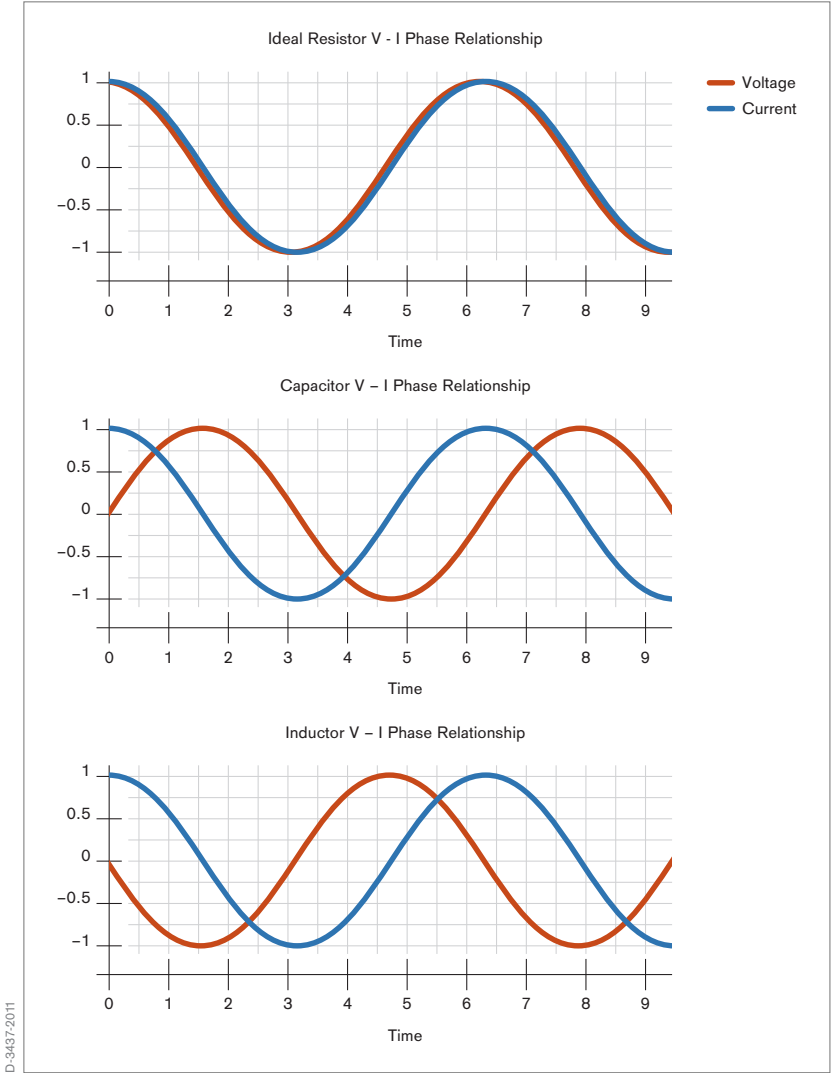
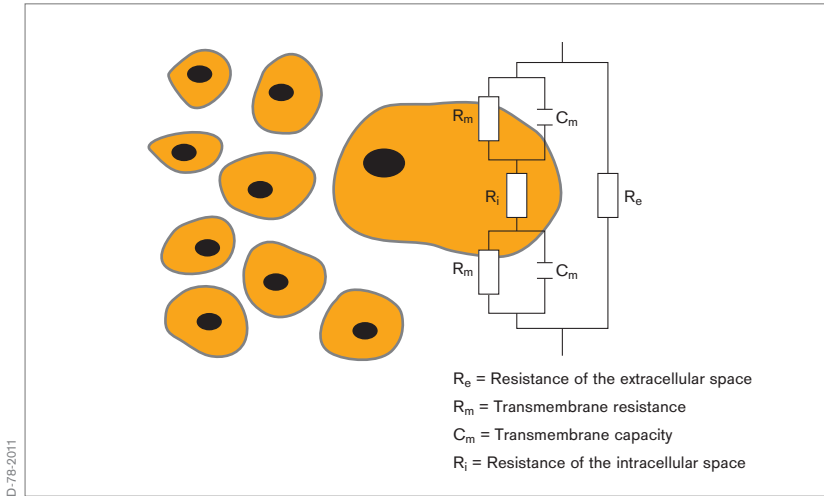Fig. 53: V-I phase relationships of resistors, inductors and capacitors

D-3437-2011

Fig. 54: Equivalent circuit diagram of biological tissue

BIOIMPEDANCE

Bioimpedance is a term used to describe the response of a living organism to an externally applied alternating electric current. It is a measure of the opposition of biological tissue to the flow of that electric alternating current.

The living organism mainly consists of cells of various different structures and the extracellular fluid which is located in the interstitial space.

With regard to bioelectric properties, biological tissue can be thought of as a complex microscopic network of electrical circuits. As the structures of adjacent cells act as trans-membrane capacitors, biological tissue has, in addition to its resistive properties, a capacitance as well, which is illustrated in Fig. 54.

As in the electric circuits described above, the bioelectrical properties of a specific tissue depend on the frequency of the applied alternating current.

The transition from a microscopic to a macroscopic view leads to a simplified electrical circuit (Fig. 55), where the specific tissue impedance is simulated by a parallel connection of a capacitor C and a resistor R_0 - R_{00}.

It can be mathematically expressed with the following formula:

$$Z = R_{00} + \frac{R_0 - R_{00}}{1 + j\omega(R_0 - R_{00})C}$$

R_{00} = Skin resistance
R_{0-00} = Specific tissue resistance
C = Specific tissue capacity
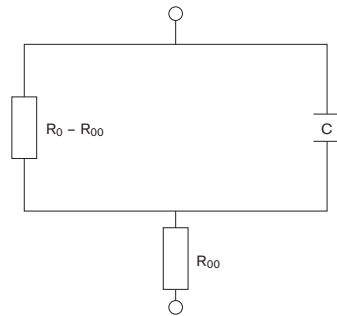
Fig. 55: Simplified equivalent circuit diagram of biological tissue

While the capacity depends on characteristics of the biomembranes of a specific tissue (ion channels, fatty acids, gap junctions, etc.), its resistance mainly depends on characteristics of the extracellular fluid (e.g., composition and amount).

Consequently, it is the specific composition (e.g., lipids, water, electrolytes in the extracellular fluid) of biological tissue which leads to distinct impedance characteristics.

Increased extra-cellular water content, high concentration of electrolytes, large cells, and a high number of cell connections via gap junctions reduce impedance (e.g., in blood and muscle). In contrast, fat accumulation, bone, and air act as electrical resistors and thus increase regional impedance. Regional impedance can be predicted by tissue resistivity (Table 1) [61].

Although in vivo measurements of electrical properties of specific biological tissues are not easily obtained and depend heavily on the experimental setup, impedance values for specific types of biological tissue can be found in the literature [15, 62, 63].

Tissue		Impedance / Resistivity
Blood		150 Ω * cm
Lung	expiration	700 Ω * cm
	inspiration	2400 Ω * cm
Fat		2000-2700 Ω * cm
Bones		16600 Ω * cm
Muscle	longitudinal	125 Ω * cm
	transversal	1800 Ω * cm
Heart Muscle	longitudinal	160-575 Ω * cm
	transversal	420-5200 Ω * cm

When bioimpedance measurements are performed to assess the lung function, the deviations between end-inspiratory and end-expiratory electrical properties are of particular interest. It is misleading to explain the increased end-inspiratory impedance by the fact that air as such is a poor electric conductor. In contrast to X-rays, the pathways of electrical current never pass through the air inside the bronchi, alveoli or pathological structures such as emphysema bulla or a pneumothorax.

The explanation for the concomitant increase of bioimpedance with increasing pulmonary air content was delivered by Nopp et al. [64, 65]: With increasing air content, the cellular structures of the lung parenchyma are
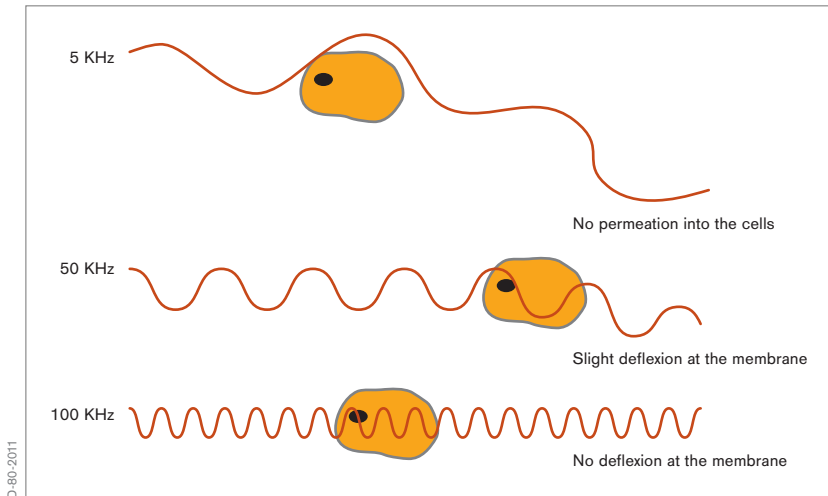
Fig. 56: Pathways of electrical current at different frequencies

stretched, increasing the length of the pathways while the diameter of the conducting cellular structure decreases.

According to the formula Z = L/S, where L is the length and S the section of a conductor, the impedance increases during inflation as the conductive cellular structures are stretched.

The electric current only passes through either intracellular or extracellular structures, depending on the frequency applied (Fig. 56).

At frequencies below 5 kHz, electrical current does not permeate into the cells and thus flows only through extracellular fluid. The tissue therefore shows mainly resistive characteristics.
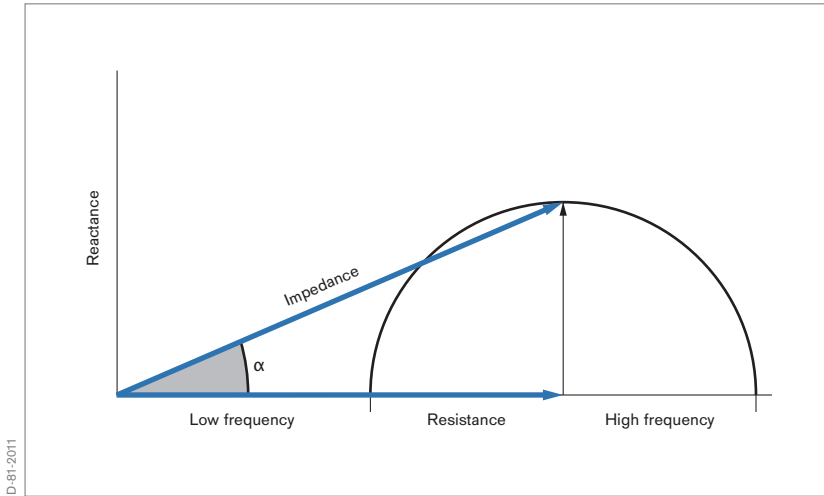
Fig. 57: Cole-Cole plot

The capacitive behavior increases with increasing frequencies and reaches its maximum at about 50 kHz. Electrical currents are slightly deflected at the cell membranes.

At higher frequencies (> 100 kHz), the electrical current is directly passing the cell membranes, resulting in a decrease in the capacitive behavior. As early as 1949, Kenneth S. Cole und Robert H. Cole described a model which explains this tissue specific impedance behavior (Fig. 57).

BIOIMPEDANCE MEASUREMENTS WITH PULMOVISTA 500

PulmoVista 500 utilizes alternating currents with a range of 80 – 130 kHz. It generally applies the current at a single frequency, which is automatically adjusted if a high level of electromagnetic background noise of a certain frequency would result in compromised data acquisition.

In contrast to bioelectrical impedance analyzers (BIA), which utilize the frequency dependent responses of the tissue to determine body composition, PulmoVista 500 requires only a single frequency to determine ventilation or cardiac related impedance changes.

PulmoVista 500 is processing the absolute magnitude of impedance; however the information on the phase difference between voltage and current is not used for signal processing.

Within the frequency range of 80 – 130 kHz, the selection of the operating frequency does not have a substantial impact on the results of the measurements or the displayed information.

Since many years, patient monitors use bioimpedance measurements to monitor respiratory function. Like with PulmoVista 500, these patient monitors also make use of the fact that trans-thoracic impedance, which in this case is measured using ECG electrodes, increases in proportion to the intra-thoracic air content, which in turn is linked to the respiratory efforts of the patient.

CARDIAC RELATED IMPEDANCE CHANGES

The thoracic impedance changes related to cardiac activity are of the same interest as those brought about by ventilation. Typically, ventilation related impedance changes of the entire electrode plane are about 10 times higher than cardiac related impedance changes. However it has to be taken into account that this ratio depends very strongly on the position of the electrodes relative to the heart, the lung water content, tidal volumes, stroke volumes and the end-expiratory lung volume, the latter suggesting that PEEP settings also will affect this ratio.

The underlying mechanisms of these cardiac related impedance changes are not completely understood.

The best explanation developed so far may be that, due to the contraction of the heart muscle during systole, low conductive lung tissue replaces high conductive heart volume. Simultaneously, lung tissue is displaced by the stroke volume distributed into the pulmonary circuit. Thus, the decrease in regional bioimpedance induced by perfusion would be a spatial dislocation effect of lung tissue caused by the expansion of major vessels and increased blood perfusion [61].

As typical tidal volumes in adults are about 500 to 600 ml and corresponding stroke volumes 70 ml, a rough correlation to the aforementioned 10:1 ratio of ventilation to cardiac related impedance changes is suggested, and actually can often be found in EIT data.

It requires further fundamental research and validation studies before information on cardiac activity or even lung perfusion derived from EIT data can be used for clinical decision making.

Appendix III: Glossary

TERM	ABBREVIATION	EXPLANATION
Acute Lung Injury	ALI	A severe, heterogeneous lung disease caused by a variety of direct and indirect issues. It is characterized by inflammation of the lung parenchyma leading to impaired gas exchange, non cardiogenic pulmonary edema, low lung compliance with concomitant systemic release of inflammatory mediators causing inflammation, hypoxemia and frequently resulting in multiple organ failure. Acute Lung Injury is defined as [66]: – Bilateral pulmonary infiltrates on chest x-ray – Pulmonary Capillary Wedge Pressure < 18 mmHg (2.4 kPa) – PaO_2/FiO_2 <300
Acute Respiratory Distress Syndrome	ARDS	A more severe form of ALI. Acute Respiratory Distress Syndrome is defined as [66]: – Bilateral pulmonary infiltrates on chest x-ray – Pulmonary Capillary Wedge Pressure < 18 mmHg (2.4 kPa) – PaO_2/FiO_2 <200

TERM	ABBREVIATION	EXPLANATION
Acute Respiratory Failure	ARF	Inadequate gas exchange by the respiratory system, with the result that arterial oxygen and/or carbon dioxide levels cannot be maintained within their normal ranges.
Alternating Current	AC	A current, in which the movement of electric charge periodically reverses direction. The usual waveform of an AC is a sine wave.
Alveolar Recruitment		Alveolar recruitment describes the process of expanding collapsed parts of the lung over the entire ventilation cycle. It is one of the primary goals of respiratory care for acute lung injury. It is aimed at improving pulmonary gas exchange and, even more important, at protecting the lungs from VILI.
Atelectasis		A condition where alveoli are deflated and collapsed, it may be due to a blockage of airways, and or, excessive external pressure on the alveoli.

TERM	ABBREVIATION	EXPLANATION
Barotrauma		The damage to the lung caused by overdistension of alveoli due to excessive trans-pulmonary pressure during mechanical ventilation. Recent clinical data demonstrate that excessive tidal volumes, and not airway pressure, is the causal factor of VALI.
Change of End-Expiratory Lung Impedance	ΔEELI	Absolute impedance measurements cannot directly be related to the end-expiratory lung impedance. However, ΔEELI closely correlates with changes of end-expiratory lung volume of the electrode plane. The parameter ΔEELI as determined by PulmoVista 500 expresses deviations of the regional end-expiratory lung impedance in relation to the global tidal variation.
Chest X-Ray	CXR	A radiograph (frontal plane) of the chest used to diagnose conditions affecting the chest. Chest radiographs are among the most common films taken, being diagnostic of many conditions.

TERM	ABBREVIATION	EXPLANATION
Computed Tomography	CT, CAT	A medical imaging method employing tomography created by computer processing. CT is one of the most important methods of radiological diagnosis. It delivers non-superimposed, cross-sectional images of the body, which can show smaller contrast differences than conventional X-ray images. For lung imaging, CT images allow to differentiate between ventral and dorsal regions of the lung.
Cyclic Opening and Closing		Describes alveoli which are collapsed at the end of expiration and open during inspiration. This condition can cause VALI. Synonymously used with the term "tidal recruitment"
Cytokines		Cytokines are substances released by cells of the immune system; they act as messengers between cells in the generation of an immune response. Lung cytokines can be released because of inadequate ventilator settings especially in patients with ALI and ARDS. An immune response triggered by cytokine activity may contribute to multiple system organ failure.

TERM	ABBREVIATION	EXPLANATION
Dependent Lung Regions		Area of the lungs, where the weight of the lung (and the heart) above this area acts as an additional weight, causing superimposed pressure. In supine position, the dependent lung regions are located in the dorsal part of the lung.
Differential Image		Is designed to display changes between two EIT images at different points in time. As these changes can generally be positive or negative, the zero value (representing no change) is always displayed in the mid-position of the colour scale, which uses -in contrast to the colour scale for Dynamic and Status Images- a turquoise colour for positive and an orange colour for negative changes.
Dorsal	D	Related to the position of the subject's spine, in EIT imaging the lower aspect of the image represents the part closest to the subject's spine. When the EIT image is subdivided into 4 layers, the dorsal part is represented by ROI 4.

TERM	ABBREVIATION	EXPLANATION
Dynamic Image		Continuously displays relative impedance changes induced by ventilation within the electrode plane as a series of tomograms. The relative impedance changes are referred to the end-expiratory impedance level.
Electrode Plane		The lens shaped intra-thoracic volume whose impedance changes contribute to the generation of EIT images. This plane is 4 cm thick at the periphery and increases towards the central region.
Electron Beam Computed Tomography	EBCT	An experimental, specific form of CT in which the X-ray tube is not mechanically spun in order to rotate the source of X-ray photons. This different design was explicitly developed to better image heart structures which never stop moving, performing a complete cycle of movement with each heart beat.
End-Expiratory-Lung Impedance	EELI	End-expiratory lung impedance, which closely correlates with end-expiratory lung volume of the electrode plane. Thus ΔEELI represents the change in end-expiratory lung volume within the electrode plane.

TERM	ABBREVIATION	EXPLANATION
End-Expiratory-Lung Volume	EELV	Sometimes synonymously used with the term FRC. However, mechanically ventilated patients exhale against PEEP rather than ambient pressure which is why physicians use the term EELV (End-Expiratory Lung Volume) instead of FRC. EELV (resp. FRC) describes the air volume which can contribute to gas exchange between two breaths. Adequate PEEP settings during mechanical ventilation help to keep alveoli and airways open thus maintaining a sufficient EELV.
Frame		A set of 208 voltage measurements taken after one complete rotation of the current injection, which is used to reconstruct one single EIT image.
Frame Rate		The frame rate is the frequency expressed as images per second at which Dynamic Images are generated.
Functional EIT	fEIT	PulmoVista 500 performs functional EIT, meaning that it mainly displays relative impedance changes as a result of lung function, i.e., ventilation and changing end-expiratory lung volume.

TERM	ABBREVIATION	EXPLANATION
Functional Residual Capacity	FRC	Physiological parameter, which describes the volume of air present in the lungs at the end of passive expiration (against ambient pressure).
Global Tidal Variation	TVglobal	The parameter TV global represents the difference between the minimum value and the maximum value in the Global impedance waveform for each breath. Regardless of the tidal volume this figure is always 100%, it solely serves as a reference for the ROI tidal variations.
Hyperinflation		See Overdistension.
Impedance		Electrical impedance, or simply impedance, describes a measure of opposition to alternating current (AC). Lung tissue during end of inspiration causes more opposition to the current than during end of expiration, and thus the intra-thoracic impedance changes with ventilation.

TERM	ABBREVIATION	EXPLANATION
Magnetic Resonance Imaging	MRI	A medical imaging technique most commonly used in radiology to visualize detailed internal structure and function of the body. MRI provides much greater contrast between the different soft tissues of the body than CT, making it especially useful in neurological, musculoskeletal, cardiovascular, and oncological imaging.
Mid-dorsal	MD	An EIT imaging specific term, referring to the part of the image that is located above the dorsal aspect. When the EIT image is subdivided into 4 layers, the mid-dorsal part is represented by ROI 3.
Mid-ventral	MV	An EIT imaging specific term, referring to the part of the image that is located below the ventral aspect. When the EIT image is subdivided into 4 layers, the mid-ventral part is represented by ROI 2.
Minute Image		The Minute Image represents regional distribution of impedance changes over the last minute. The Minute Image displays Tidal Images averaged over the last minute.

TERM	ABBREVIATION	EXPLANATION
Multiple Inert Gas Elimination Technique	MIGET	An experimental technique used mainly in pneumology, that involves measuring mixed venous, arterial, and mixed expired concentrations of six infused inert gases. In many cases MIGET yields the crucial information about the physiology of gas exchange, i.e. shunt, dead space, and the general ventilation versus blood flow (Va/Q).
Non-dependent Lung Regions		Area of the lungs without superimposed pressure. In supine position, the non-dependent lung regions are located in the ventral part of the lung.
Overdistension		Excessive expansion of the lungs at the end of inspiration. Recent findings suggest, that overinflation is the predominantly cause of VILI. Often synonymously used with Overinflation and Hyperinflation. According to L. Gattinoni [1], in CT images lung regions with Hounsfield Units from -900 to -1000 are classified as overdistended. In EIT data, the effects of overdistension can only indirectly be seen, as overdistended lung regions have a low compliance and are thus less ventilated. Further studies are required to validate the capability of EIT to directly detect overdistension.

TERM	ABBREVIATION	EXPLANATION
Overinflation		See Overdistension.
Positive End Expiratory Pressure	PEEP	The pressure during mechanical ventilation used to oppose passive emptying of the lung and to keep the airway pressure above the atmospheric pressure. PEEP is used to maintain a sufficient end-expiratory lung volume.
Pulmonary Consolidation		The solidification of normally aerated lung tissue, that occurs as a result of accumulation of inflammatory cellular exudate in the alveoli and adjoining ducts. Consolidation may also occur due to the alveolar space filling with water or blood.
Pulmonary Shunt		Pulmonary shunt describes alveoli that are perfused but not ventilated, e.g. due to collapse or consolidation.

TERM	ABBREVIATION	EXPLANATION
Recruitment Maneuver	RM	A procedure, usually performed with a mechanical ventilator, aimed at expanding collapsed lung tissue. In order to recruit collapsed lung tissue, sufficiently high peak pressures and PEEP levels must be temporarily imposed to exceed the critical opening pressure of the affected lung region. After the recruitment maneuver the PEEP must be kept high enough that subsequent de-recruitment does not occur. Recruitment maneuvers also have a time related component as the time required to open (heterogeneous) alveoli varies.
Region of Interest	ROI	A user-defined area within an EIT status image. The image can be divided horizontally or into quadrants. In PulmoVista 500, the area covered by each ROI is represented by a corresponding regional impedance waveform, a TV ROI and a regional ΔEELI.
ROI Tidal Variation	TV ROI	Regional Tidal Variations show the percentage of ventilation related impedance change which takes place in the corresponding ROI.

TERM	ABBREVIATION	EXPLANATION
Single Photon Emission Computed Tomography	SPECT	An experimental, nuclear tomographic imaging technique using gamma rays. Similar to CT, it delivers cross-sectional images of the body.
Status Image		A Tidal Image or Minute Image;
Tidal Image		The Tidal Image represents regional distribution of impedance changes of the last detected breath. The Tidal Image is a differential image of the end of inspiration compared to the beginning of inspiration.
Tidal Recruitment		See Cyclic Opening and Closing.
Tomogram		A cross-sectional image, created by a tomograph.
Tomograph		A device, used to create a tomogram.
Tomography		A method of producing a cross sectional image, in slices, of a solid object.
Transverse Plane		PulmoVista 500 provides cross-sectional images as if looking through the subject's feet, the left side of the image represents the right side of the subject.

TERM	ABBREVIATION	EXPLANATION
Ventilator Associated Lung Injury	VALI	Lung injury as a result of mechanical ventilation, caused by either excessive (regional) tidal volumes leading to overdistension and / or cyclic opening and closing of alveoli as a result of insufficient PEEP settings. In relation with mechanical ventilated patients, the term VALI has replaced the term VILI, as clinical data show that preexisting lung injury seems to be mandatory for the observed adverse effects of mechanical ventilation.
Ventilator Induced Lung Injury	VILI	Sometimes used synonymously with VALI, but correctly the term VILI should only be used in the context of a purposely induced lung injury in laboratory settings.
Ventral	V	Related to the position of the subject's sternum (or belly), in EIT imaging the upper aspect of the image, regardless of whether the patient is lying in supine, lateral or prone position. When the EIT image is subdivided into 4 layers, the ventral part is represented by ROI 1.

TERM	ABBREVIATION	EXPLANATION
Volutrauma		The damage to the lung during mechanical ventilation, caused by excessive (regional) tidal volumes leading to overdistension of alveoli It is not necessarily associated with barotrauma: the pressure in the alveoli may not be excessive but they may still be overdistended.

D-3415-2011

Eckhard Teschner, born in 1964 in Bremen, has a biomedical engineering background, but also worked in emergency care and the intensive care environment. After his studies, he was occupied as Senior Product Manager in the business fields of radiology, cardiology and heart surgery. He joined Dräger in 1999 and was the responsible Product Manager for the EIT technology project since it was initiated in 2001 in cooperation with the EIT group Göttingen.

He has initialized and accompanied various scientific and clinical cooperations with international experts in lung mechanics and mechanical ventilation. He has been present during more than 100 EIT measurements on intensive care patients which partly had severe respiratory dysfunctions.

In the product development process of PulmoVista 500, he has specified its product requirements and designed its graphical user interface.

D-70-2011

Prof. Dr. med. Michael Imhoff is board certified in general surgery and intensive care medicine. Research areas include trauma surgery, intensive care medicine, patient monitoring, clinical data management, artificial intelligence in medicine and health economics, leading to over 300 publications and scientific presentations.

He teaches Medical Informatics and Statistics at the Ruhr-University Bochum, Germany, is a reviewer for the German Research Foundation, a member of the editorial boards of and reviewer for several international biomedical journals, and chairman of the section for patient monitoring of the German Association of Biomedical Engineering (DGBMT).